Measurements and modeling of VLLE at elevated pressures

Laursen, Torben

Publication date:
2002

Document Version
Early version, also known as pre-print

ISBN 87-90142-81-0
Printed by Book Partner, Nørhaven Digital, Copenhagen, Denmark

Preface

This thesis is submitted as partial fulfillments of the requiments for obtaining the Ph.D. degree in chemical engineering at the Technical University of Denmark, Lyngby, Denmark. The work presented in this thesis has been carried out from august 1999 to June 2002 in the research group: Center for Phase Equilibria and Separation Processes (IVC-SEP) at the Department of Chemical Engineering, Technical University of Denmark. The work has been supervised by Associate Professor Simon Ivar Andersen and Associate Professor Peter Rasmussen. I would like to express my gratitude and thank my supervisors for their inspiration and fruitful discussions and productive collaboration.

Further, I am very grateful to Professor R.B. Heidemann, at the University of Calgary, Canada, for giving me the opportunity to work in his group for 6 months in order to work in the modeling of the then obtained data.

_____

Torben Laursen

Abstract

The analysis of multiphase systems at elevated pressure is of great interest both from an academic side and an industrial point of view. The literature contains limited data for such systems, and the measurement of the composition of the different phases of multiphase systems at elevated pressures has traditionally been considered very time consuming. This work aims at developing and operating an equipment which allows routine measurements of both VLE and VLLE, in the temperature range of 25-45°C and pressure range of 1-100 bar. This has been done by taking advantage of on-line sampling and pure component calibration. Samples from the different liquid phases in the high-pressure cell is taken using a moveable needle. The systems investigated have been a combination of the components: CO_2, N_2, di-methyl ether (DME), water, methanol, ethanol and 1-propanol. 41 isotherms have been measured and of these 18 were VLLE systems and 32 have not previously been published.

Some of the experimental results have been modelled using an equation of state, SRK combined with the MHV1 mixing rule for the a-parameter and the NRTL model for the Gibbs excess energy. The Mathias-Copeman model was used in the expression for the pure-component a-parameter. For all the involved binary pairs the interaction parameters, τ_{ij}, for the NRTL model were fitted to experimental data with the α-parameter fixed at 0.2. The obtained model has showed very good results when used to predict multi component VLE and VLLE systems containing CO_2, while the model has some problems with systems containing N_2.

Abstract in Danish

Termodynamiske studier af multifase systemer ved højere tryk er af stor interesse for både den akademiske og den industrielle verden. Til trods for det, indeholder litteraturen få experimentielle datasæt for sådanne systemer, og disse målinger anses for at være meget kostbare og tidskrævende. Dette projekt havde som mål at udvikle og anvende apparatur som tillader rutinemålinger af både VLE og VLLE systemer i temperatur området 25-45°C og trykområdet 1-100 bar. Dette er blevet opnået ved at anvende on-line prøveudtagninger og kalibering vha. de rene komponenter. Prøverne fra de forskellige væskefaser er blevet udtaget via en bevægelig nål.

De undersøgte systemer har været en kombination af komponentene: CO_2, N_2, di-methyl ether (DME), vand, methanol, ethanol and 1-propanol. 41 isothermer er blevet målt, af disse er 18 VLLE systemer og 32 er ikke tidligere blevet målt.

Nogle af de eksperimentielle datasæt er blevet modelleret med en tilstandsligning: SRK, kombineret med MHV1 blandingsreglen for a-parametren og NRTL modellen for excess Gibbs energien. Mathias-Copeman modellen er blevet brugt i udtrykket for ren-komponent a-parametren. For alle de binære par er interaktionsparametren τ_{ij}, for NRTL modellen tilpasset eksperimentielle data, mens α-parametren er blevet fastsat til 0.2. Den opnåede model er i stand til at forudsige VLE og VLLE systemer med CO_2, mens den har problemer med at give en god forudsigelse for systemer med N_2.

Table of Content

1 Introduction

The analysis of multiphase systems at elevated pressure is of great interest both from an academic side and an industrial point of view. But despite of this, the amount of data in the literature is limited. Not only have a large number of systems not been measured at all, but for those systems where experimental data are available, the range of composition, temperature and pressure is limited for most of the systems. The reason for this is that experimental work is generally considered very time consuming and very expensive. As a reaction to this much research effort has centered on the development of models that would be able to correlate and predict phase behaviour based on limited experimental data, or "experimental" data are simulated on a computer. In this project great emphasis has been put in developing equipment that would allow both VLE and VLLE systems to be measured on a routine basis, providing inexpensive, reliable and fast access to experimental data.

Most time has been gained by using pure-component calibration of the GC, as opposed to using calibration by mixtures of known composition. This means that the calibrations can be done in between sampling from the cell, reducing the workload of calibration for a binary system from 3-5 full working days to 2 hours, and since these 2 hours are placed in between sampling from the cell, no measurement time is wasted on calibration. For systems with more than two components even more time is saved. Using this approach it is possible to measure between 8 and 13 data points, including sampling from all the phases in the used cell in a week. In other words, one full isotherm can be measured per week.

In this project the systems measured has been composed of the components: N_2, CO_2, di-methyl ether (DME), water, methanol, ethanol and 1-propanol. The reason that these components were chosen is that a Danish company: Haldor Topsøe A/S, has been looking into the possibilities for large scale production of DME. They do not have N_2 in there systems, but instead H_2. But since H_2 is difficult to treat experimentally has been replaced with N_2. Systems with ethanol and 1-propanol were measured after all the

measurements for Haldor Topsøe was finished in order to see if using a larger alcohol would have any significant effect on the phase equilibria.

The project also contains a model part, but since the experimental work has evolved successfully, it was decided to give the model work a lower priority. Therefore only during a six months stay in Canada was fulltime work done in trying to model the obtained data. Despite the limited time spent on the modelling work, very good and promising results have been obtained. It has been shown that multiphase multi component systems can be modelled using an equation of state combined with an excess Gibbs energy model. As for the experimental part a simplistic approach has been taken. The chosen model is SRK combined with the Mathias-Copeman expression for the pure-component a-parameter, the MHV1 mixing rule for the a-parameter and the NRTL model for the excess Gibbs energy. For each binary pair the two interaction parameters of the NRTL model were fitted while keeping the α-parameter fixed to 0.2.

2 Part I: Experimental methods

This section gives the general principles of the used experimental methods.

The equipment used in this project was acquired by the IVC-SEP several years before the start of this project. Therefore the basic design was fixed, but a large number of minor changed to the equipment was done in order to be able to reproduce litteratur and own datasets.

2.1 Layout of equipment

Figure 1 shows a diagram of the used equipment:

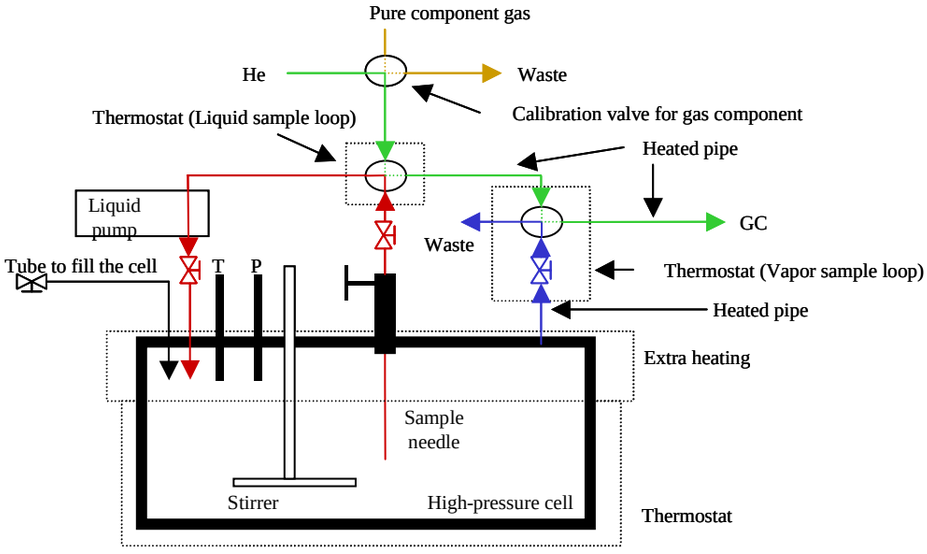

Figure 1: Sketch of the used equipment.

The center of the setup is the cell. The cell can withstand a pressure of 250 bar, but has not been exposed to a pressure above 110 bar due to five o-rings in the cell. The reason for this, is that o-rings tend to break when exposed to light gases at high pressures. As an example, the cell would always leak after being exposed to CO_2 at 100 bars. Mixing in the cell is done mechanically by a stirrer. The cell is equipped with two windows, giving

the user a good view of the content of the cell. Since the windows are placed in the middle of the cell, it can be difficult to see the bottom and top of the cell.

2.2 Thermostating

The thermostating of the original cell delivered by TOP Industries, France, was done using 4 heating rods mounted into the sides of the cell, and a PT100 thermometer mounted into a well in the lid, placing it in the middle of the cell. The settings are electronically controlled. After some time it was discovered that the thermostating of the cell was not properly designed since when operated at temperatures above 35°C "rain" was seen in the cell. This was due to the lack of heating in the top of the cell, giving the lid a slighter lower temperature than the rest of the cell, yielding condensation on the inside of the lid. The problem was solved by adding extra heating to the lid.

2.3 Sampling

Both the liquid and the vapor sample is taken on-line and is sent directly into the gas chromatograph, GC, using the He-stream, green color in Figure 1. The liquid sample-loop is 0.5 μL, and is mounted in the line connecting the sampling needle with the circulation pump, red color in Figure 1. A liquid sample is taken by first placing the needle in the liquid phase that is to be analyzed. The pump is switched on and is let to run for at least two minutes while it is checked visually that it is running. Letting it run for two minutes makes sure that the sample loop is 100% flushed by the liquid. Then the pump is switched off and the sample loop is turned and the sample enters into the GC via the He-stream.

The vapor sample is taken from a hole in the lid that is connected to a on/off valve and a 500μL sample loop, blue color in Figure 1. The line between the valve and the loop is heated well above the cell temperature. This has to be done to make sure that no condensation occurs from the vapor, leading to wrong measurements. When a sample is taken, it is first made sure that the line and loop is properly heated. Then the valve is opened slightly until a small stream of gas comes out from the sample valve. An amount of gas is let out until the loop is flushed by the vapor. As for the liquid sample the vapor sample is sent directly into the GC via the He-stream.

2.4 Calibration of the GC

In order to determine the composition of the samples sent into the GC, the GC has to be calibrated so that the peak area can be related to composition. This can be done using two methods:

- Mixture calibration
- Pure component calibration

Mixture calibration is done by preparing a number of mixtures of known composition that are sent to the GC. Based on the peak areas, a calibration curve can be made. This method is very time consuming, since preparing the mixtures takes long time.
Pure component calibration is done by injecting different amounts of the pure component, yielding a calibration curve relating amount in gram with peak area. This is done for each component, and when a sample is analyzed the area for each component is converted to moles using the calibration curves and then the composition is easily calculated.
Pure component calibration has two major advantages over mixture calibration:

- Time: Preparing mixtures is very time consuming and the time spent grows significantly with the number of components in the system.
- Composition: It can be difficult to measure the right amount of each compound since small amounts are used in a heavy sample cell.
- Uncertainty: The time span between the calibration and the actual measurements is large yielding a added uncertainty to the measurements, since the signals of the GC tend to drift.

The basis of this project has been the use of pure component calibration.

On the used GC with the applied thermo coupling detector TCD, it was found that all calibration curves were slightly non-linear. And they were all fitted to the equation:

$$amount = a \cdot (peak\ \ area)^{b} \tag{1}$$

The two parameters a and b were fitted to the data, and all fits would yield an R^2 better then 0.999.

2.5 Calculation of pure component density

The method requires the knowledge of the density of the compound either as gas or as liquid.

Density of liquids

For all the liquid components the liquid density was taken from DIPPR [DIPPR, 1989], see equation 2 and Table 1:

$$density\left[g/cc\right] = \frac{M}{1000} \cdot \frac{A}{B^{\left(1+\left(1-\frac{T}{C}\right)^{D}\right)}} \tag{2}$$

In equation two, M is the molar mass, and T is the temperature in kelvin.

Component	A	B	C	D
Water	5.459	0.30542	647.13	0.081
Methanol	2.288	0.2685	512.64	0.2453
Ethanol	1.648	0.27627	513.92	0.2331
1-propanol	1.235	0.27136	536.78	0.24

Table 1: Constants used to calculate liquid density [DIPPR, 1989]

Density of gases

For the three gases different methods were used. For DME and N_2 the viral equation of state truncated after the first term (B), was used. While for CO_2 interpolation of experimental data from the literature was used.

The density of DME was taken from [Haworth and Sutton, 1971], using the expression:

$$density\left[g/cc\right] = M \cdot \frac{P}{RT + BP} = 46.06 \cdot \frac{1}{82.06 \cdot T - 456} \tag{3}$$

Here M is the molar mass, P is pressure, R is the gas constant, T is temperature in kelvin and B is the second viral coefficient [Haworth and Sutton, 1971]. The atmospheric pressure is taken as 1 atm. Please note that B is not used as a function of temperature, since the value of B is small compared with the factor RT in equation 3.

The density of N_2 was calculated using also the second viral coefficient that was taken from [Duschek, 1988], using the expression:

$$density\left[g/cc\right] = M \cdot \frac{P}{RT + BP} = 28.014 \cdot \frac{1}{82.06 \cdot T - 5.94} \qquad (4)$$

Please note that as for DME B is not taken as a function of T since the value of B is small compared with the factor RT in equation 4.

Note that both DME and N_2 is close to an ideal gas.

The density of CO_2 was taken from [Angus, 1979]. The equation used for the density was found by fitting the values given in [Angus, 1979] first to the pressure to obtain values for 1 atm and then to the temperature. The values used are given in Table 2:

T [K]	P [bar]	
	0.95	1.0
290	0.00174 [g/cc]	0.00184 [g/cc]
300	0.00168 [g/cc]	0.00177 [g/cc]

Table 2: Density values taken from [Angus, 1979], used to obtain a fit of the density of CO_2

Table 2 shows that the density of pure CO_2 shows some changes with pressure, indicating that taking the atmospheric pressure as a constant value of 1 atm gives a contribution to the error of the calibration of CO_2. This error is considered so small that it is not taken in to account.

The resulting equation is:

$$density\left[g/cc\right] = 0.003768 - 6.7385 \cdot 10^{-6} \cdot T\left[K\right] \quad (5)$$

Here T is the room temperature in kelvin around the calibration loops used.

Figure 2-4 shows two calibration curves and the resulting isotherm for the system: CO_2/DME, the reading for the liquid phase and the vapor phase are indicated on the calibration curves. As can be seen good agreement is obtained between this work and literature data.

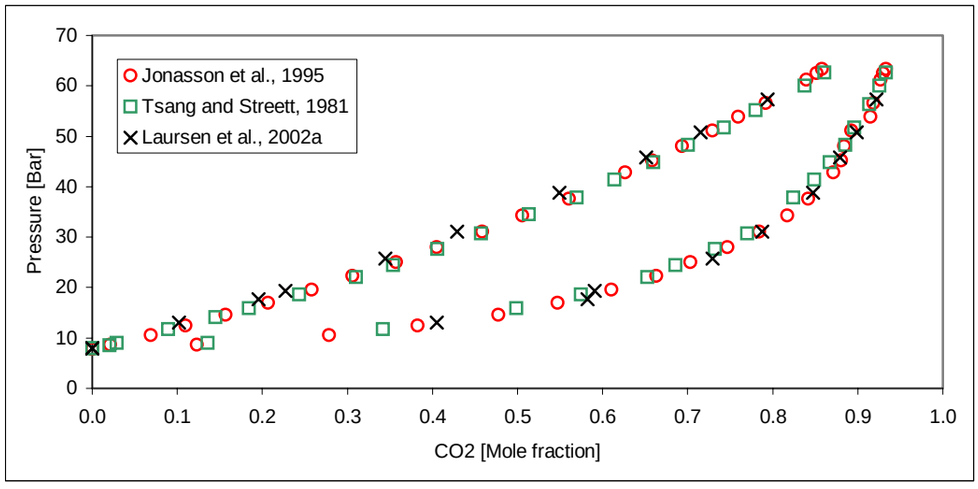

Figure 2: Comparison of literature data and data from this project, for the system: CO_2/DME, T=35.0°C

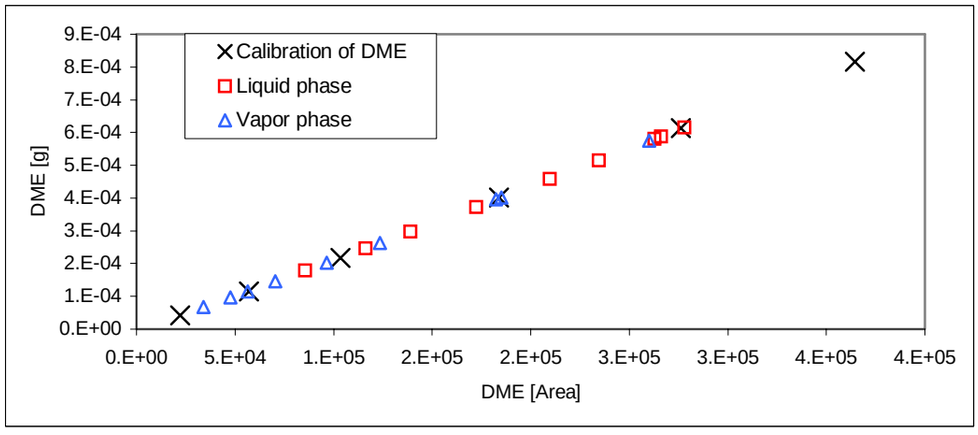

Figure 3: Calibration curve for DME, including values used for figure 2

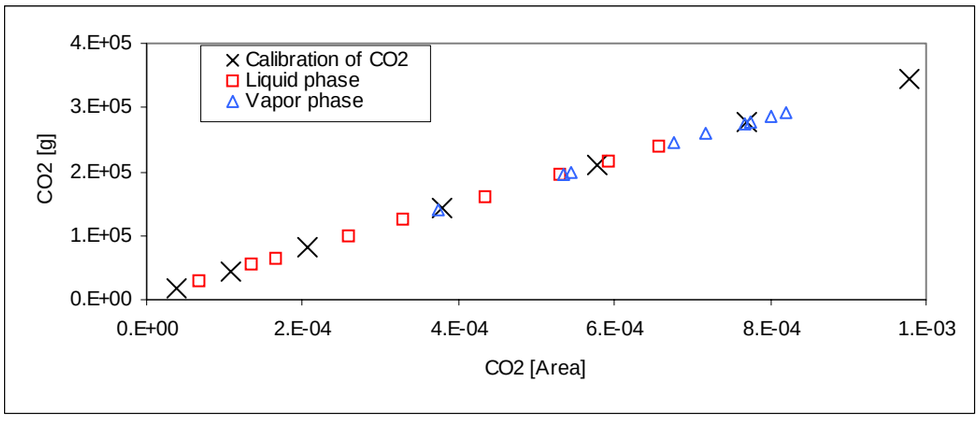

Figure 4: Calibration curve for CO_2.

2.6 Uncertainty of data

For each data point the uncertainty is composed of several contributions:

- Temperature of the cell
- Pressure in the cell
- Impurity of the used chemicals
- Detector of the GC (peak area)
- Calibration of the used GC

Temperature

The temperature in the cell was found to be well controlled within ±0.1 K. As noted it was found necessary to add additional heating to the lid of the cell, and this means that the lid of the cell will have a slightly higher temperature then the rest of the cell. Several systems were measured, CO_2/DME, N_2/DME, CO_2/methanol and they compare well with literature data. It is therefore believed that this temperature gradient in the cell does not have any significant contribution to the uncertainty.

Pressure

Pressure was found to be controlled within 0.2 bar. When taking a vapor sample from the cell, gas was removed from the cell, and depending on the gas in the cell, N_2 or CO_2, and the pressure in the cell, that will lead to a pressure drop in the cell between 0.1 and 2 bar. There were always taken two samples from the vapor, so when the second sample was taken the pressure would be lower than when the first sample was taken. Since the two vapor samples taken from the cell would always be highly reproducible, 1-2% AAD., this pressure drop is not believed to have any significant contribution on the uncertainty of the data.

Impurity of the chemicals used

All the used chemicals were of analytical purity, and were used without further purification. During a part of the project problems with polluted DME were

encountered. It was found that the bottles that the DME was supplied in were polluted with a polymer that was transferred to the equilibrium cell with the DME. Since the cell has a number of o-rings made of a polymer, meaning that any mixture in the equilibrium cell will always be in contact with a polymer, it is believed that this pollution did not have any effect on the equilibria in the cell. The problem was solved by switching to a different DME container.

Detector of the GC (peak area)

The used GC has the problem that it gives a very noisy baseline. The used GC was equipped with both particle and O_2 filter, the problem was therefore believed to arise from the detector itself. Due to the old age of the GC, it was not possible to repair it.

The noisy baseline means that when integrating the peaks, this always has to be done manually. The integration method used was always baseline to baseline. The noise on the baseline has no significant effect on large peaks, but when integrating small peaks, the area obtained was very sensitive to where the baseline was drawn. This has only an effect when integrating the peaks from the heavy components in the vapor phase, and the mole fraction given for these components therefore has a very large uncertainty. This uncertainty has been estimated to be around 30%. This is a very large number compared with what normally is seen in the literature, but it has to be remembered that these numbers only apply to the smallest mole fractions measured, in the range of 0.001 mole fraction.

Another problem with the detector is that the signal has a drift, that is the signal from the same amount of compound will change over time. Figure 5 shows a run test that was done using N_2:

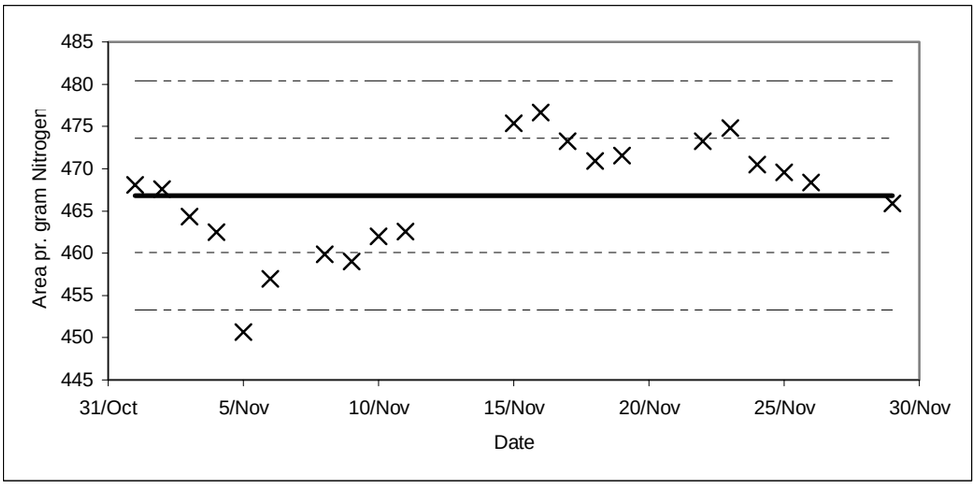

Figure 5: Results of run test done on the used GC using N_2.

As Figure 5 shows the detector does have a significant drift in the signal when injecting the same amount of N_2. The drift has not been measured for any other compounds, but it is expected that they will all have a similar drift.

This shows that the lifetime of a calibration is limited, and should be done as close together with the VLE/VLLE measurements as possible, and at best in-between sampling from the cell. Exactly this method has been used in this project.

3 Part II: Experimental results

This section gives a overview of all the experimental results obtained in this project. All the results have either been published or submitted for publication in Journal of Chemical Engineering Data. See reference [Laursen et al, 2002a,b,c] and appendix A, B, C for details. The data are arranged according to the three series in which they were measured. All data values have been placed in the appendices as copies of the published or submitted articles. This part of the thesis therefore consists mostly of Figures with the data. Table 3 gives a overview of the systems measured in this project, the temperatures and the number of data points:

System	Type	Temperatures, °C, (Number of data points)
Data published [Laursen et al., 2002a], see appendix A		
N_2/DME	VLE	25.0 (11), 35.0 (11), 45.0 (12)
CO_2/DME	VLE	25.0 (6), 35.5 (10), 47.0 (11)
CO_2/CH_3OH	VLE	25.0 (6), 30.0 (7), 40.0 (5)
N_2/DME/H_2O	VLLE	25.0 (6), 35.0 (8), 45.0 (6)
CO_2/DME/H_2O	VLLE	25.0 (6), 35.0 (5), 45.0 (6)
N_2/DME/H_2O/CH_3OH	VLLE	25.0 (6), 35.0 (7), 45.0 (6)
CO_2/DME/H_2O/CH_3OH	VLLE	25.0 (5), 35.0 (5), 45.0 (5)
N_2/CO_2/DME/H_2O/CH_3OH	VLLE	25.0 (7), 35.0 (6), 45.0 (6)
Data accepted for publication [Laursen et al., 2002b], see appendix B		
N_2/CH_3OH	VLE	25.0 (8), 35.0 (8), 45.0 (8)
Data submitted for publication [Laursen et al., 2002c], see appendix C		
CO_2/DME/ethanol	VLE	25.0 (8), 35.0 (8), 45.0 (8)
N_2/DME/H_2O/ethanol	VLE	25.0 (6), 35.0 (6), 45.0 (7)
CO_2/DME/H_2O/ethanol	VLLE	25.0 (6), 35.0 (7), 45.0 (7)
CO_2/1-propanol	VLE	35.0 (10), 45.0 (11)
CO_2/DME/1-propanol	VLE	25.0 (6), 35.0 (7), 45.0 (7)

Table 3: Overview of the measured data

3.1 1. series of measurements

All the measurements of the 1. series have been published [Laursen, et al., 2002a]. The main conclusion of this work is that it is possible to measure both VLE and VLLE on a routine basis. Also it is shown that systems with DME and water can form both VLE and VLLE systems together with other components. See appendix A for more information.

Included in this article are also measurements of the systems CO_2/DME and CO_2/methanol, which were measured to verify that the used method was valid and could be used to reproduce literature data. For one other measured system, N_2/DME, deviation between this method and literature data was found [Teodorescu and Rasmussen, 2001], see Figure 6:

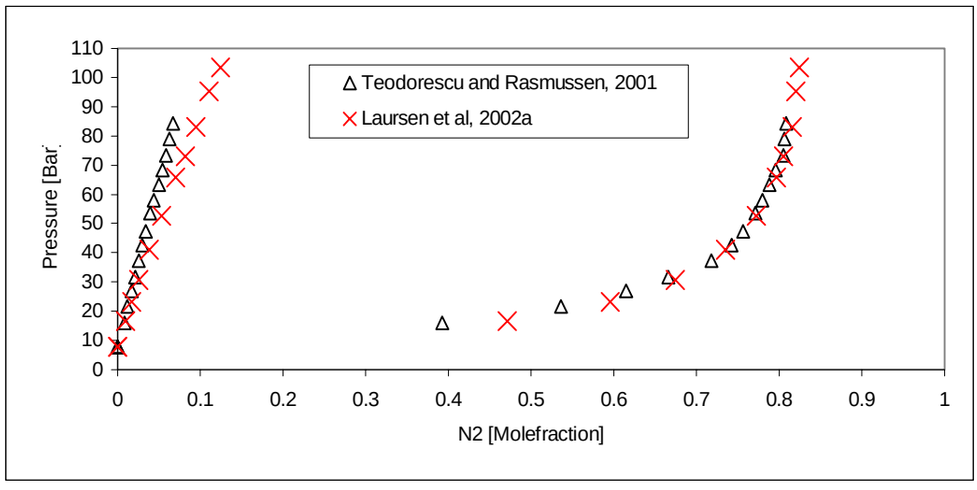

Figure 6: Example of disagreement between this work and literature data, T=35.0°C

No explanation could be found for the difference in the liquid phase composition, but it should be noted that the measurements were done using a different equipment and using mixture calibration of the GC. The sampling method was the same, and the setup of the used GC was also the same. The only main difference was the calibration used and the integration of the GC-peaks. In this work a PC based software was used: ChemStation from HP, while in the other work a paper integrator was used. In order to verify that our method was valid the isotherm was remeasured, see Figure 7:

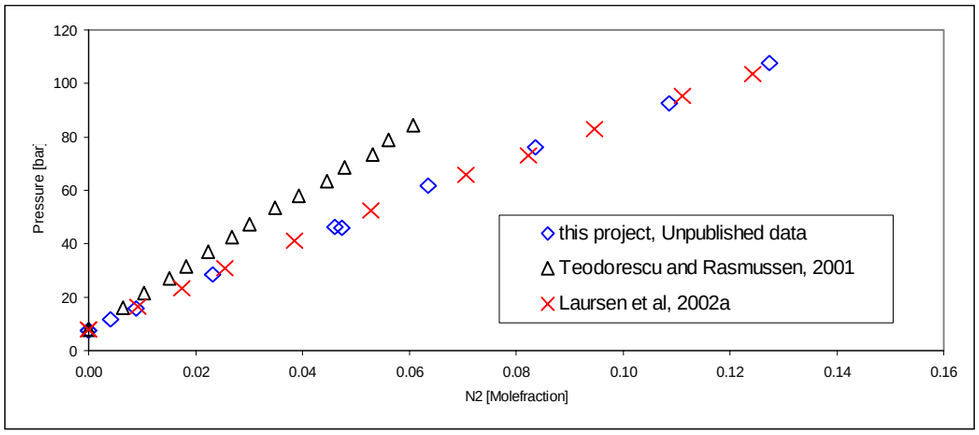

Figure 7: Comparison of the liquid phase composition for the system: N_2/DME

As Figure 7 shows, the data was well reproduced in this work, this does not verify the accuracy of the data, but does show that the method used is reproducible.

One of the most interesting part of this work was the new ability of measuring VLLE systems. The first VLLE system to be measured was CO_2/DME/H_2O, see Figure 8

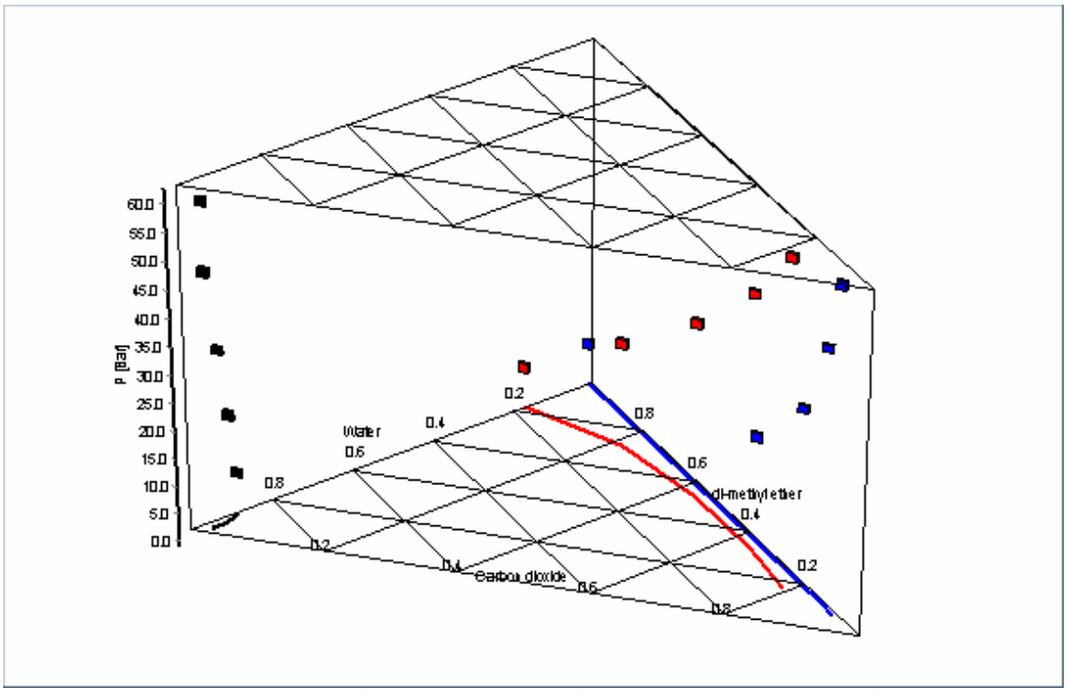

Figure 8: 3D plot of the system CO_2/DME/H_2O, T=35.0°C

Figure 8 is a 3D plot of the composition as the triangle with the pressure as the 3. dimension. The measured points are shown both as points in 3D and as a projected line

onto the 2D composition space. Black colour indicates the water rich liquid phase, red colour is the DME rich liquid phase, while the blue colour is the vapor phase.

The system would start as a two component VLLE system, and as CO_2 was added and the pressure raised, the upper liquid phase would expand, and the measurements were stopped when the system was close to becoming an LLE system.

Next the VLLE system: N_2/DME/H_2O was measured, see Figure 9. This system showed no major change in either of the liquid phases as N_2 was added and the pressure raised. The only change was seen in the vapor phase where N_2 would replace DME.

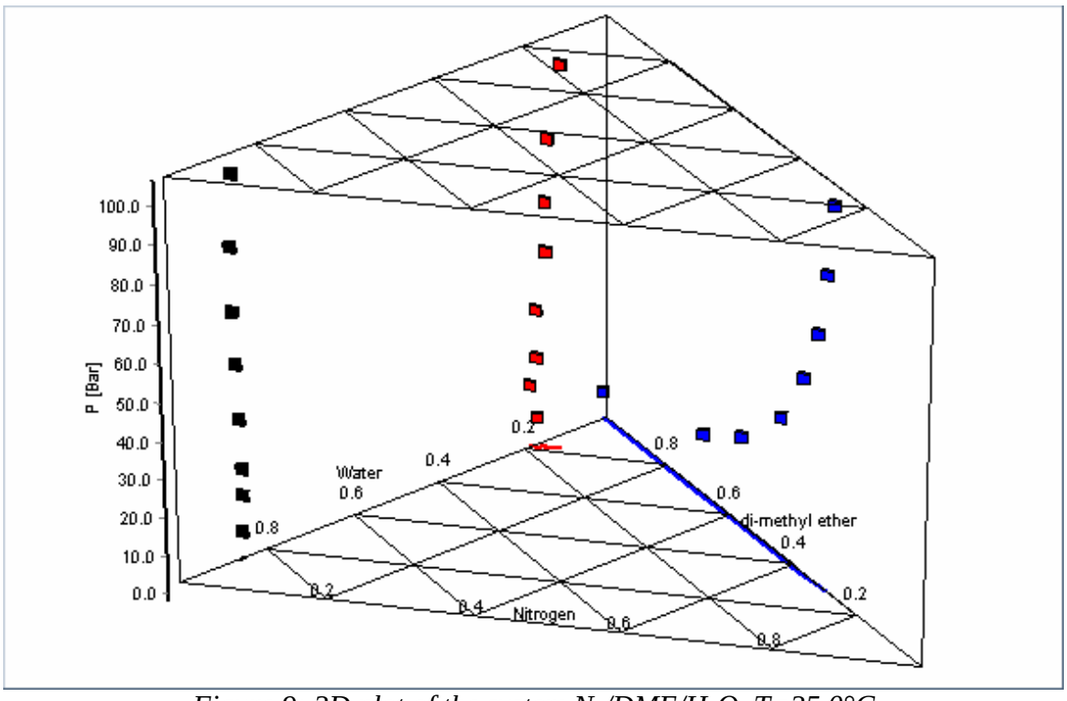

Figure 9: 3D plot of the system N_2/DME/H_2O, T=35.0°C

In addition the system N_2/DME/H_2O, showed a very small temperature effect, see Figure 10.

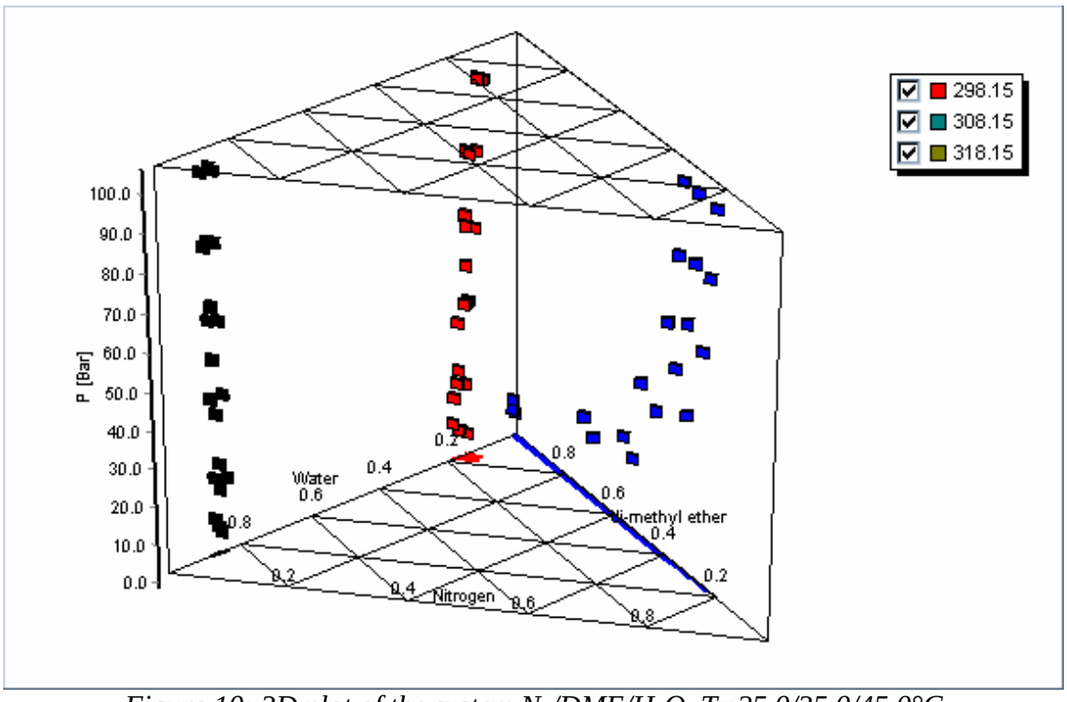

Figure 10: 3D plot of the system N_2/DME/H_2O, T=25.0/35.0/45.0°C

3.2 2. series of measurements

These sets of data have been accepted for publication [Laursen et al., 2002a]
The aim of the work was to measure the system: N_2/methanol, where no literature data was found for both the liquid and the vapor phase. The system was measured at three temperatures: 25, 35, 45 °C and up to 100 bars.
All relevant information has been inserted in the accepted article, see appendix B.

3.3 3. series of measurements

After finishing the measurements of systems with methanol, it was decided to measure some systems with ethanol and 1-propanol in order to see if increasing the size of the alcohol would have any marked effect of the behavior of the systems. This was found not to be the case. These sets of data have been submitted for publication [Laursen et al., 2002c], see Appendix C.

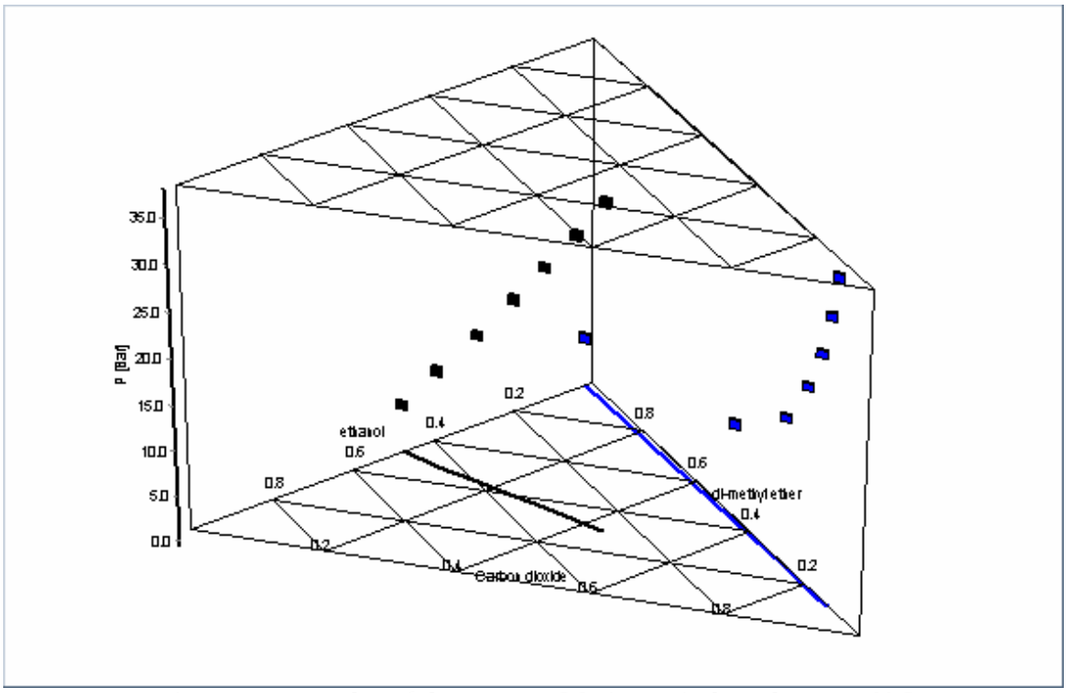

Figure 11: 3D plot of the system CO_2/DME/Ethanol, T=35.0°C

Figure 11 shows how the CO_2 enters the system, and moves the system closer to the critical point where the system becomes a one phase system. This is seen in the cell as an expansion of the liquid phase. The measurement are stopped when only a small amount of vapor phase can be seen in the cell.

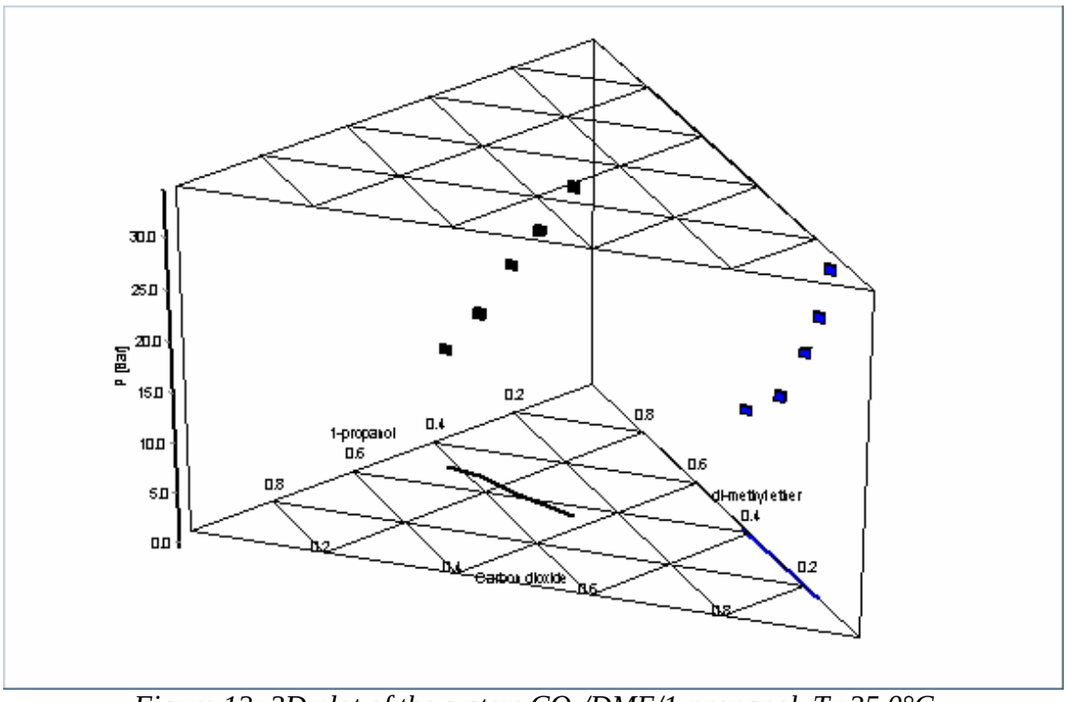

Figure 12: 3D plot of the system CO_2/DME/1-propanol, T=35.0°C

Figure 12 shows the system as in Figure 11, but here ethanol has been replaced with 1-propanol. As can be seen there is no marked effect of increasing the size of the alcohol.

4 Part III: Theoretical results

4.1 Introduction

The modeling work done has been divided into three parts based on the three series of measurements, see table 2.

1. series of measurements

These datasets have all been modeled, see below for details.

2. series of measurements

These datasets have been correlated with the Soave-Redlich-Kwong equation of state (SRK) [Soave, 1972] fitting the k_{ij} parameter, see appendix B for details

3. series of measurements

No attempt has been made to model these datasets.

All the calculations were done using the in-house simulation software SPECS version 3.0, 2000, IVC-SEP, Department of Chemical Engineering, The Technical University of Denmark, Denmark.

4.2 Modeling of the first series of data

The aim of this work was to try if the VLE and VLLE data from the 1. series of measurements could be modelled using a equation of state combined with a model for the excess Gibbs energy. The binary interactions parameters will be fitted to experimental data and the obtained model used to predict the multicomponent multiphase systems using a multiphase flash.

4.2.1 Model used

Initially several models were tested in order to investigate which model to use. But only one model was used to perform all the modeling.

All work was based on the SRK equation of state:

$$P = \frac{RT}{V-b} - \frac{a(T)}{V(V+b)} \tag{6}$$

using a linear mixing rule for the b-parameter:

$$b = \sum_{i=1}^{N} z_i b_{ii} \tag{7}$$

Using for the pure b-parameter:

$$b_{ii} = \frac{2^{1/3}-1}{3} \cdot \frac{RT_{ci}}{P_{ci}} \tag{8}$$

and for the pure a-parameter:

$$a_{ii} = \frac{1}{9(2^{1/3}-1)} \cdot \frac{R^2 T_{ci}^2}{P_{ci}} [F]^2 \tag{9}$$

Two models for the temperature dependence of α was tested.
The original expression using the acentric factor [Soave, 1972]:

$$F = 1 + \left(0.480 + 1.574\omega_i - 0.176\omega_i^2\right)\left(1 - \sqrt{T_{ri}}\right) \tag{10}$$

And the Mathias-Copeman expression [Mathias and Copeman, 1983]:

$$\begin{aligned} F &= 1 + C_1\left(1 - \sqrt{T_{ri}}\right) + C_2\left(1 - \sqrt{T_{ri}}\right)^2 + C_3\left(1 - \sqrt{T_{ri}}\right)^3, \quad T_{ri} < 1 \\ &= 1 + C_1\left(1 - \sqrt{T_{ri}}\right), \quad T_{ri} > 1 \end{aligned} \tag{11}$$

In this work the Mathias-Copeman expression was found to be the best, see Figure 13 and 14. As can be seen a significant improvement is obtained as compared to using the acentric factor:

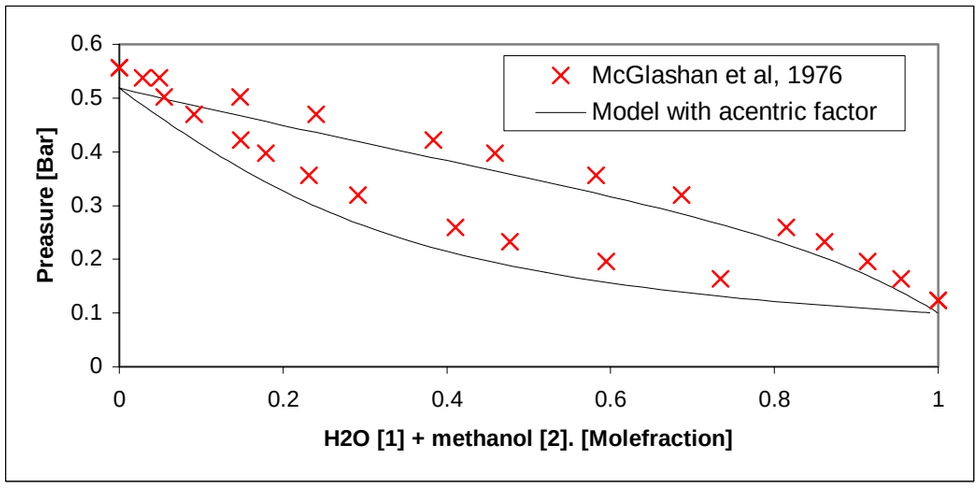

Figure 13: Fit of the system: methanol/water, using the acentric factor expression at 50.0°C.

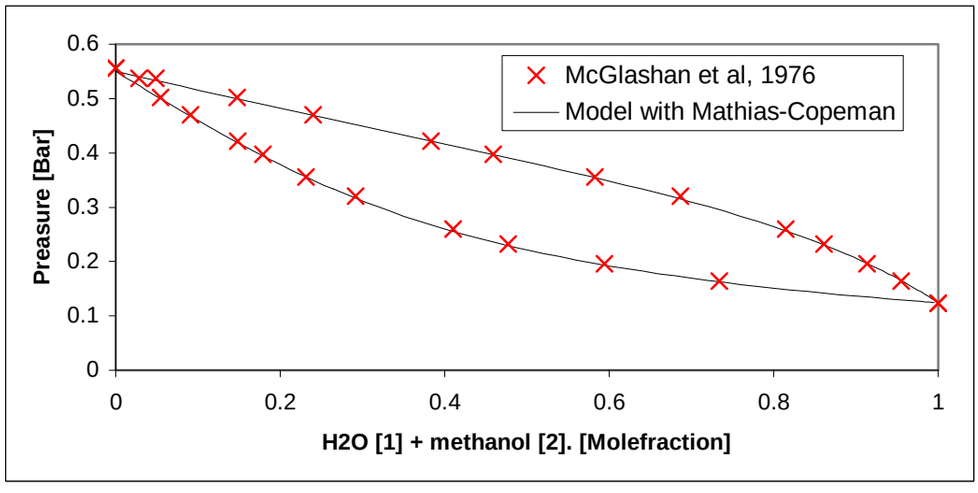

Figure 14: Fit of the system: methanol/water, using the Mathias-Copeman expression at 50.0°C.

As mixing rule for the a-parameter two models were tested, MHV1 and MHV2 [Michelsen, 1990]. Both models were found to perform similarly and the MHV1 was chosen since it has one parameter less than MHV2.

The MHV1 mixing rule can be written as:

$$\frac{a}{bRT}=\alpha_{mix}=\sum_{i=1}^{N}x_i\alpha_{ii}+\frac{1}{q_1}\left[\frac{g^E_{(P=0)}}{RT}+\sum_{i=1}^{N}x_i\ln\left(\frac{b}{b_{ii}}\right)\right],\quad q_1=-0.593 \tag{12}$$

As model for the excess Gibbs energy two models were tested: NRTL [Renon and Prausnitz, 1968] and UNIQUAC [Abrams and Prausnitz, 1975]. Both models were found to perform similarly and the NRTL was chosen since it contains fewer parameters.

The NRTL model can be written as:

$$\frac{g^E}{RT}=\sum_{i=1}^{N}\frac{n_i}{n_t}\frac{\sum_{j=1}^{N}\tau_{ji}G_{ji}n_j}{\sum_{l=1}^{N}G_{li}n_l} \tag{13}$$

With:

$$\tau_{ji}=\frac{\lambda_{ji}}{RT},\ G_{ji}=\exp\left(-\alpha_{ji}\tau_{ji}\right),\ \left(\alpha_{ji}=\alpha_{ij}\right) \tag{14}$$

The pure component constants used were taken from [DIPPR, 1989 & Dahl et al., 1991], and are given in Table 4:

	T_c [Kelvin]	P_c [MPa]	C_1	C_2	C_3	M [g/mol]
N_2	126.20	3.400	0.5427	-0.0524	-0.3381	28.014
CO_2	304.21	7.383	0.8653	-0.4386	1.3447	44.010
$(CH_3)_2O$	400.10	5.359	0.8837	-1.0352	2.8278	46.069
H_2O	647.13	22.055	1.0873	-0.6377	0.6345	18.015
CH_3OH	512.64	8.097	1.4450	-0.8150	0.2486	32.042

Table 4: Critical values, molar mass and Mathias-Copeman parameters

4.2.2 The fitting procedure

A number of different experimental data for binary systems were used to fit the interaction parameters and, depending on the data available, different objective functions were used.

If only the composition for the liquid phase were available, a bubble point P or T routine was used.

If only the composition for the vapour phase was available dew P or T was used as object function.

$$F_{OB} = \sum_{k=1}^{D} \left(\frac{P_k^{\exp} - P_k^{cal}}{P_k^{\exp}} \right)^2$$
$$R_1 = \frac{\sum_{k=1}^{D} \left(\frac{P_k^{\exp} - P_k^{cal}}{P_k^{\exp}} \right)}{D} \qquad (15)$$

$$F_{OB} = \sum_{k=1}^{D} \left(\frac{T_k^{\exp} - T_k^{cal}}{T_k^{\exp}} \right)^2$$
$$R_1 = \frac{\sum_{k=1}^{D} \left(\frac{T_k^{\exp} - T_k^{cal}}{T_k^{\exp}} \right)}{D} \qquad (16)$$

If the composition for both the liquid and vapor phase were available the objective function was the equality of the fugacity in both phases:

$$F_{OB} = \sum_{k=1}^{D} \left[\left(y_2^{\exp} \left(\varphi_1^L - \varphi_1^V \right) - y_1^{\exp} \left(\varphi_2^L - \varphi_2^V \right) \right)^2 + \left(\left(x_1^L \varphi_1^L - y_1^V \varphi_1^V \right) + \left(x_2^L \varphi_2^L - y_2^V \varphi_2^V \right) \right)^2 \right]$$
$$R_1 = \frac{\sum_{k=1}^{D} \left| y_2^k \left(\varphi_1^{L,k} - \varphi_1^{V,k} \right) - y_1^k \left(\varphi_2^{L,k} - \varphi_2^{V,k} \right) \right|}{D} \qquad (17)$$
$$R_2 = \frac{\sum_{k=1}^{D} \left| \left(x_1^{L,k} \varphi_1^{L,k} - y_1^{V,k} \varphi_1^{V,k} \right) + \left(x_2^{L,k} \varphi_2^{L,k} - y_2^{V,k} \varphi_2^{V,k} \right) \right|}{D}$$

A summary of the data used, the object function used and the resulting fits are given in table 5.

System	Data source	Data points	Model
$N_2/(CH_3)_2O$	Laursen et al., 2002a	34	R_1= 0.0039 (17) R_2= 0.0110
N_2/H_2O	Rigby and Prausnitz, 1968 Japas and Franck, 1985	13 99	R_1= 0.22% (16) R_1= 69.69% (15)
N_2/CH_3OH	Brunner et al., 1987 Krichevskii and Levedeva, 1947 Weber et al., 1984	22 21 10	R_1= 5.69% (15) R_1= 8.34% (15) R_1= 5.23% (15)
$CO_2/(CH_3)_2O$	Laursen et al., 2002a	27	R_1= 0.0047 (17) R_2= 0.0085
CO_2/H_2O	Mueller et al., 1988 Nakayama et al., 1987	14 11	R_1= 0.0076 (17) R_2= 0.0058 R_1= 0.0014 (17) R_2= 0.0148
CO_2/CH_3OH	Laursen et al., 2002a	18	R_1= 0.0014 (17) R_2= 0.0144
$(CH_3)_2O/H_2O$	Laursen et al., 2002a Pozo and Streett, 1992	12 8	R_1= 0.0030 (17) R_2= 0.0266 R_1= 0.0118 (17) R_2= 0.0286
$(CH_3)_2O/CH_3OH$	Holldorff and Knapp, 1988 Chang et al., 1982	45 45	R_1= 0.0066 (17) R_2= 0.0111 R_1= 0.0188 (17) R_2= 0.0204
H_2O/CH_3OH	Kurihara et al., 1995 McGlashan and Williamson, 1976 Hall et al., 1979 Kooner et al., 1980	58 39 10 14	R_1= 0.0055 (17) R_2= 0.0101 R_1= 0.0078 (17) R_2= 0.0164 R_1= 0.0061 (17) R_2= 0.0240 R_1= 0.0070 (17) R_2= 0.0247

Table 5: Overview over the fitted binary systems, the data used, object function used and results. Numbers in brackets indicate the objective function used.

4.2.3 Obtained parameters

The obtained parametres are summarized in table 6:

τ_{ij}	N_2	CO_2	$(CH_3)_2O$	H_2O	CH_3OH
N_2	0.0000	0.0000	-0.6844	6.1614	2.2969
CO_2	0.0000	0.0000	0.8314	11.646	2.2190
$(CH_3)_2O$	1.5656	-0.9455	0.0000	1.8583	1.4017
H_2O	4.1436	1.7852	0.8040	0.0000	1.2472
CH_3OH	-0.1449	-0.7866	-0.3808	-0.5220	0.0000
$\alpha_{ij} = \alpha_{ji}$					
N_2	0.0000				
CO_2	0.0000	0.0000			
$(CH_3)_2O$	0.2000	0.2000	0.0000		
H_2O	0.2000	0.2000	0.2000	0.0000	
CH_3OH	0.2000	0.2000	0.2000	0.2000	0.0000

Table 6: Obtained parameters for the model: MHV1 combined with NRTL

Note that the value of α was a fixed value.

4.2.4 Results for binary VLLE data

The datasets that are to be predicted by the model, contain both VLE and VLLE multicomponent systems. Therefore it is of interest to test whether the obtained model can predict VLLE behavior in these binary systems. Since a multiphase flash can not be used to find three phases in a binary system, the location of the 3-phase point was found using plots of the Gibbs energy of mixing, see Figure 15:

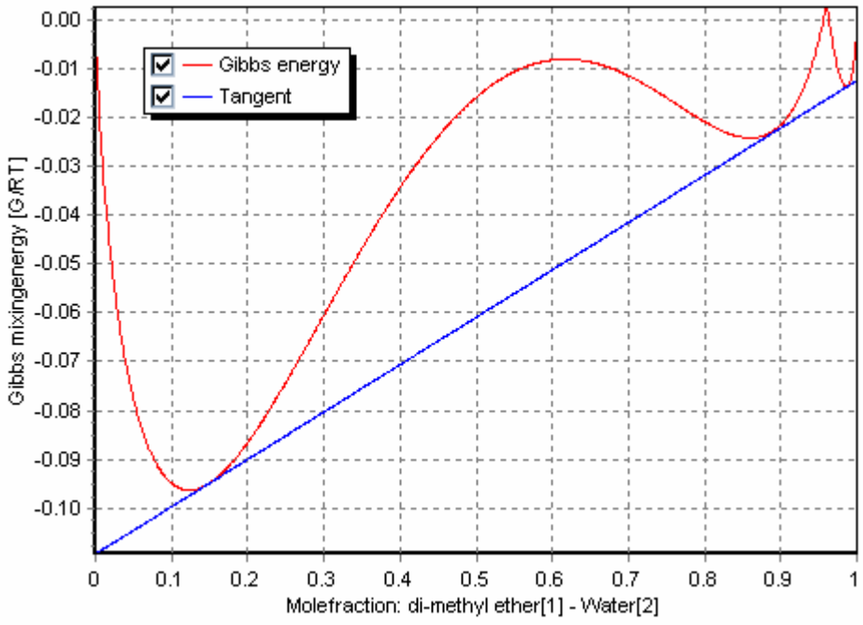

Figure 15: Plot of the Gibbs energy of mixing for the system DME + water, showing a VLLE point, T = 322.7 kelvin, P = 10.39 bar.

This method yields an uncertainty of the VLLE point temperature of 0.1 K and VLLE point pressure of 0.01 bar. The VLLE point found by the model was determined by fixing the temperature to the experimental value taken from [Holldorf and Knapp, 1988], and changing the pressure while visual inspecting the Gibbs energy plot if the VLLE point was found. Since the Gibbs energy curve is very sensitive to changes in both temperature and pressure, the read off values can be obtained with a precision comparable with experimental values.

This procedure was repeated for each of the experimental points [Holldorf and Knapp, 1988], see Figure 16:

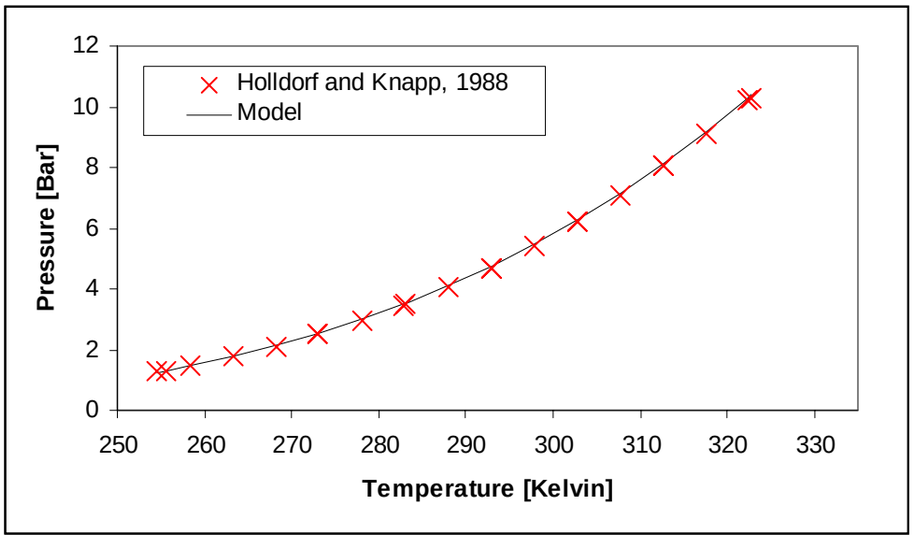

Figure 16: Plot of VLLE curve for the system DME + water

As Figure 16 shows the model does locate the correct VLLE curve over the entire experimental range.

4.2.5 Results for multi component systems

When applying the model to predict multicomponent systems, good results were obtained for systems with CO_2 but without N_2, therefore the results are divided into two parts depending on whether the systems contains N_2 or not.

The model values for the composition were obtained by using an average of the measured phase composition as feed to the TP multiphaseflash. The multiphaseflash is built into the inhouse software used: SPECS and is based on standard methods [Michelsen, 1982]. For the systems with three phases and three components the results from the flash can be compared directly with the experimental data, since the system has zero degrees of freedom when T and P are fixed. But when the number of components exceed the number of phases present in the system, the system is not fixed and the flash results can not be directly compared with the experimental values. Since the feed to the flash is an average of the experimental values, the outcome is expected to lay close.

4.2.6 Results for systems with CO_2 but without N_2

These types of multicomponent systems were modeled without many problems. The same good results were obtained at the three measured temperatures: 25, 35 ,45°C. Therefore only the results at 35.0°C are shown here in Figure 17-18. As can be seen is both the number of phases and the composition of the phases match well.

The reason that the plot for L2 in Figure 17 does not show any lines for the first point is that the flash can not find three phases for a two component system.

The plot for L1 in Figure 18 shows a large deaviation between model and data for the first point. The reason for this is that the system has one degree of freedom, but the feed was not corrected. The plot for L2 in Figure 18 showes a large deaviation between the model and the data for the first point, but the point is close to a critical point for the system and is therefore difficult to both measure and model.

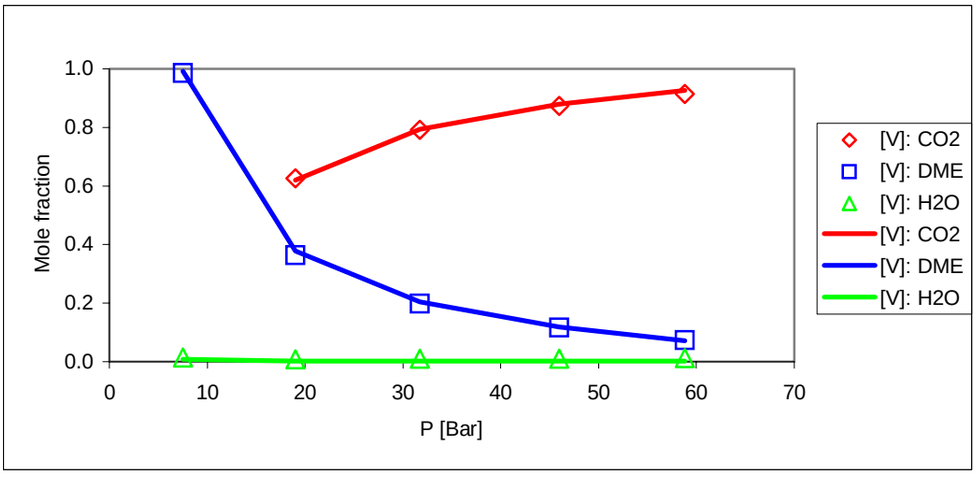

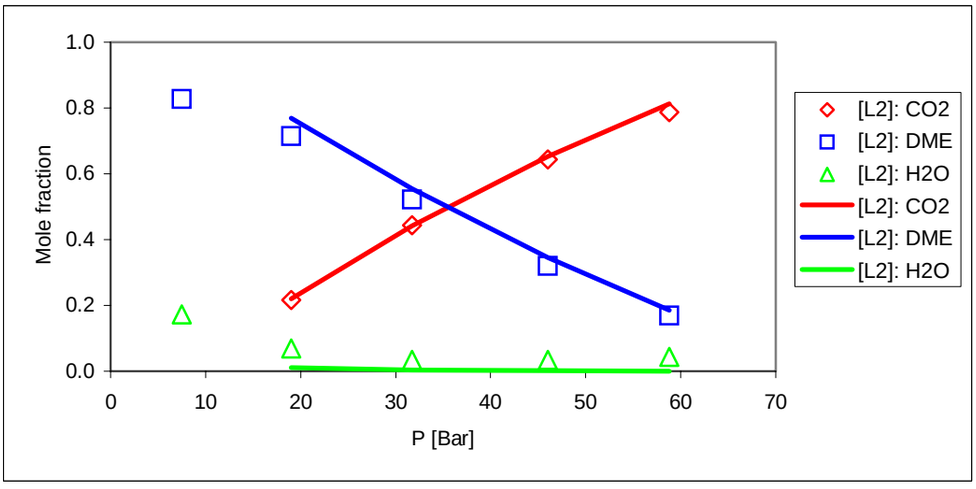

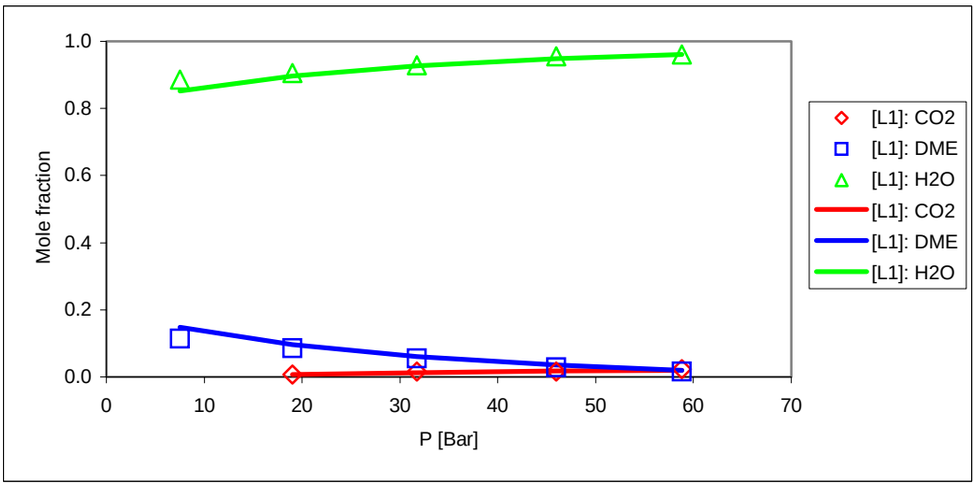

Figure 17: Plot of model + experimental data for the system: CO_2/DME/H_2O, T=35.0°C. L1: Lower liquid phase, L2: Upper liquid phase, V: vapor phase

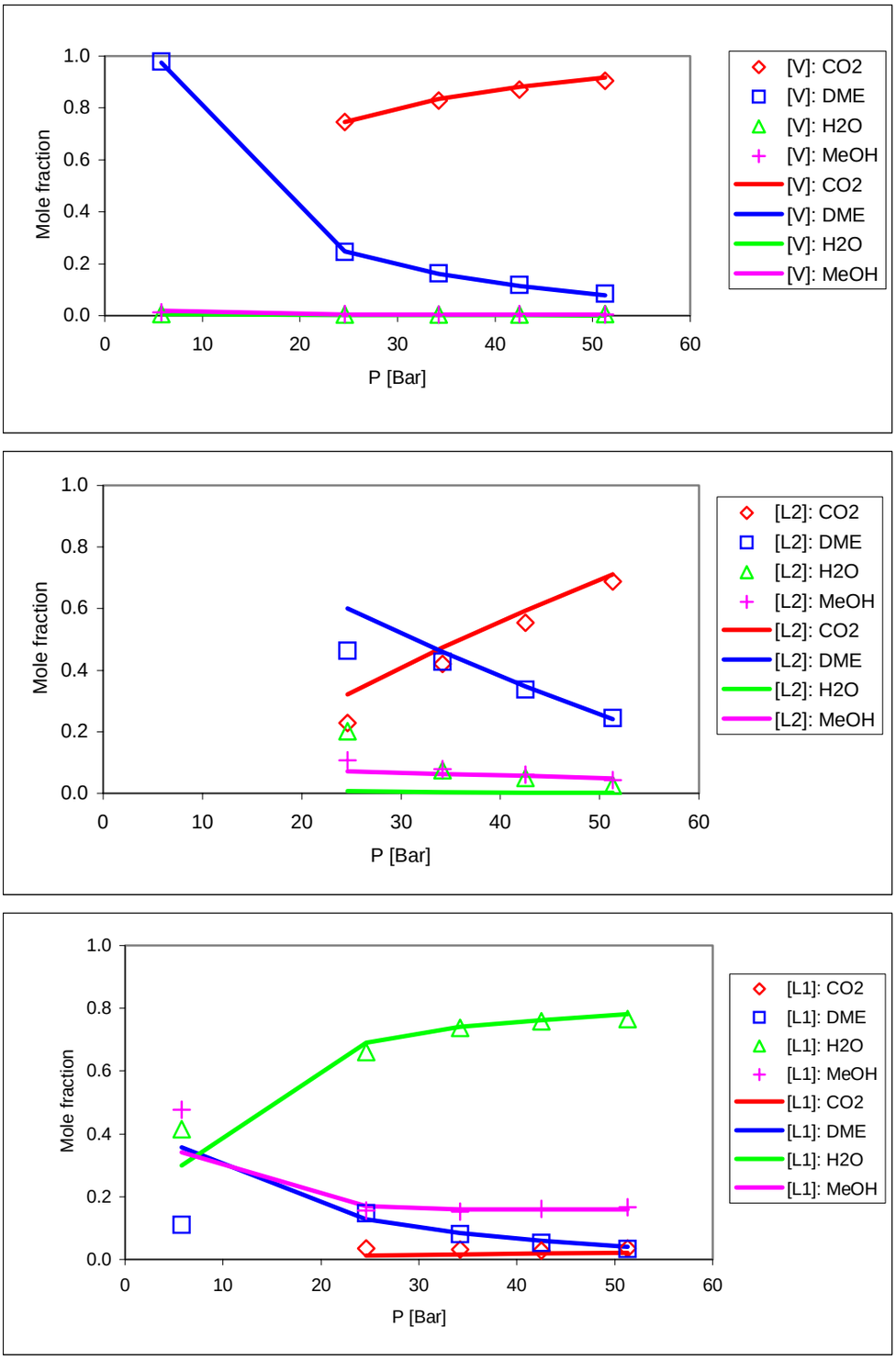

Figure 18: Plot of model + experimental data for the system: CO_2/DME/H_2O/methanol, T=35.0°C, L1: Lower liquid phase, L2: Upper liquid phase, V: vapor phase

4.2.7 Results for systems with N_2 but without CO_2

It has not been possible to obtain the same good results for systems with N_2 without CO_2, see Figure 19-20.

As can be seen is the lower liquid phase matched very well, but for the upper liquid and vapor phase there is a systematic difference. For the 4 component system: N_2/DME/H_2O/methanol in Figure 20, the model finds a second liquid phase, but this can be removed by changing the feed.

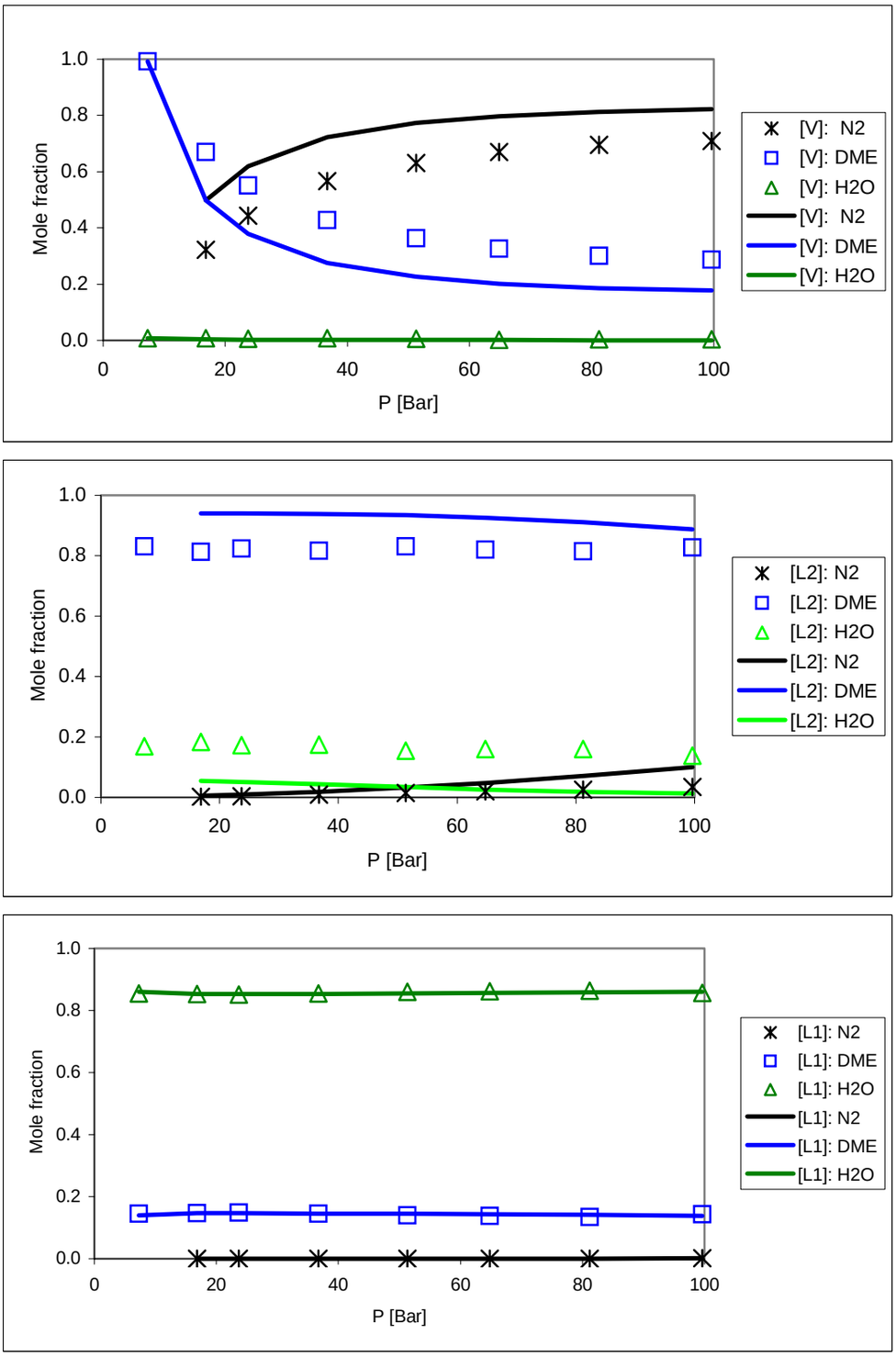

Figure 19: Plot of model + experimental data for the system: N_2/DME/H_2O, T=35.0°C
L1: Lower liquid phase, L2: Upper liquid phase, V: vapor phase

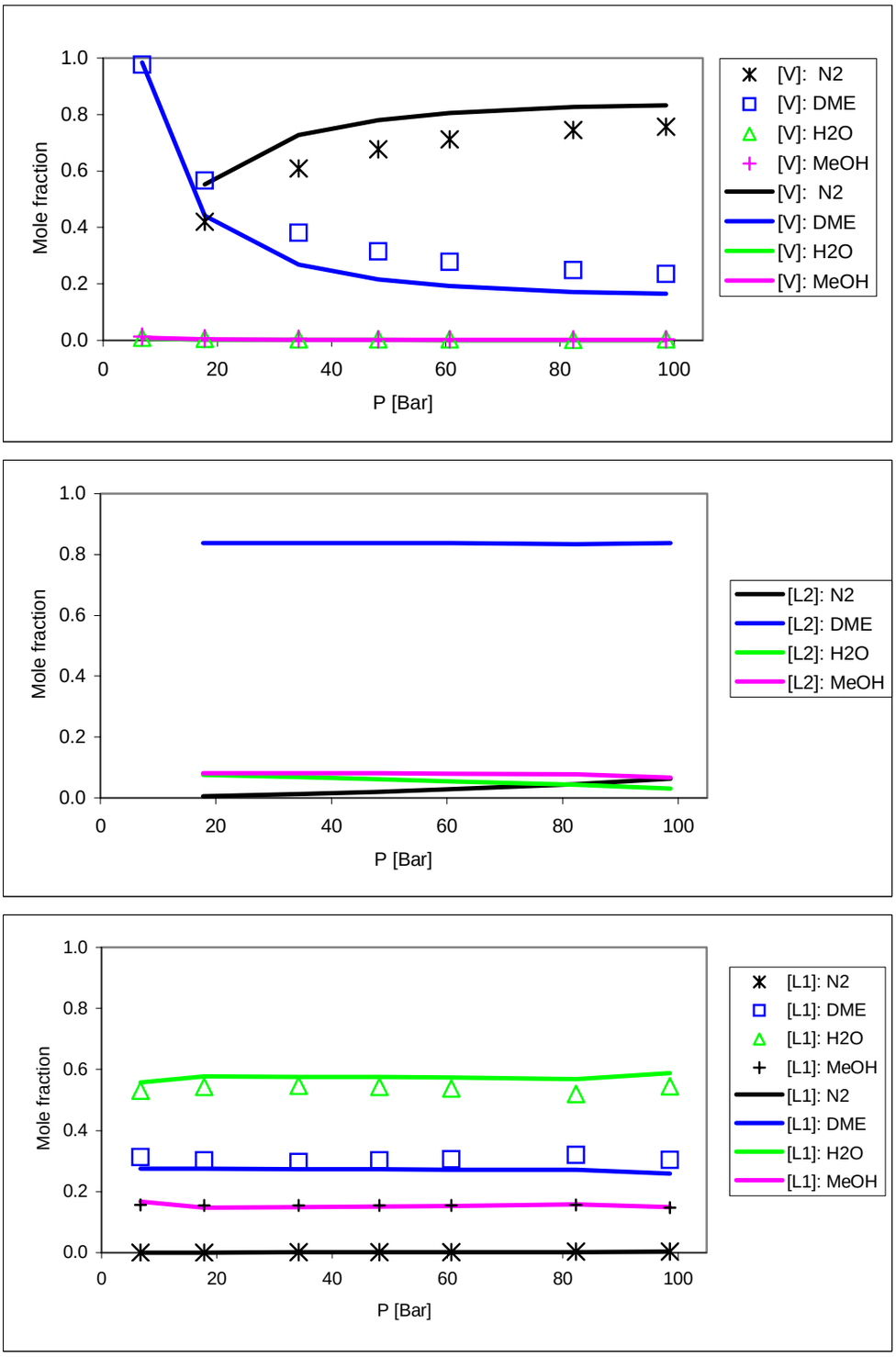

Figure 20: Plot of model + experimental data for the system: N_2/DME/H_2O/methanol, T=35.0°C, L1: Lower liquid phase, L2: Upper liquid phase, V: vapor phase

N_2 is supercritical at this temperatures and pressures, and therefore it was tried to plot the function in equation 9 to see if it showed any strange behavior, see Figure 21.

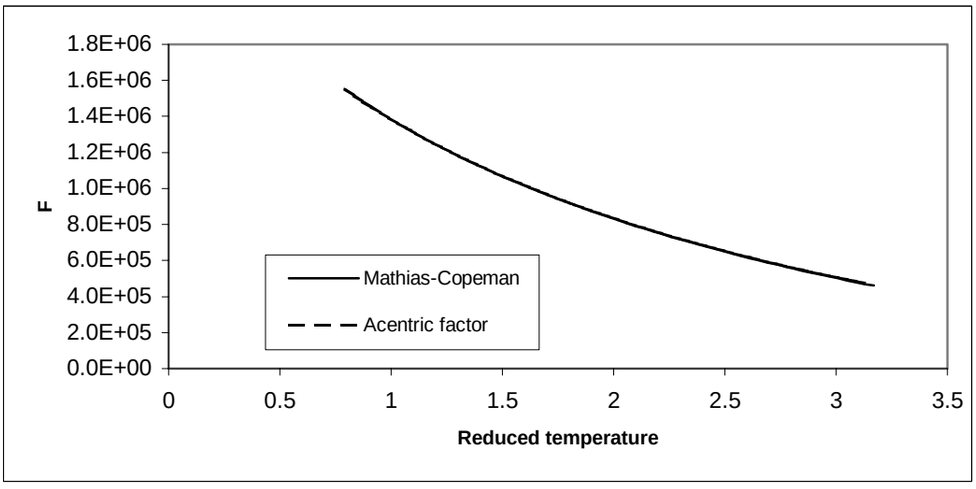

Figure 21: Plot of equation 10 and 11 for N_2 as function of reduced temperature.

Figure 21 shows that neither equation 10 nor 11 has any marked shape and gives the same results, and therefore it was tried if empirical changes to F in equation 9 could improve the results see Table 7:

Value of F in equation 9			MC	F=0.5	F=1.0	F=1.5	F=2.0
Phase	Component	Experimental					
Vapor	N_2	0.4426	0.6342	0.6341	0.6318	0.6321	0.6385
	DME	0.5514	0.3630	0.3631	0.3654	0.3651	0.3587
	H_2O	0.0061	0.0028	0.0028	0.0028	0.0028	0.0028
	Fraction		0.2269	0.2268	0.2213	0.2084	0.1774
Upper Liquid	N_2	0.0044	0.0120	0.0122	0.0215	0.0392	0.0761
	DME	0.8235	0.9003	0.9002	0.8959	0.8865	0.8629
	H_2O	0.1721	0.0877	0.0876	0.0826	0.0744	0.0610
	Fraction		0.4224	0.4225	0.4270	0.4384	0.4676
Lower liquid	N_2	0.0001	0.0001	0.0001	0.0001	0.0002	0.0004
	DME	0.1491	0.1293	0.1292	0.1268	0.1226	0.1152
	H_2O	0.8508	0.8706	0.8707	0.8731	0.8772	0.8844
	Fraction		0.3507	0.3507	0.3518	0.3532	0.3550

Table 7: Comparison between experimental values and flash results with different expressions for the function F in equation 9. P=23.7 bar, T=35.0°C

Table 7 shows that replacing the value from the Mathias-Copeman expression with a empirical value does not give any major change in the composition of the vapor phase, while the two liquid phases show minor change.

The only way found to change the calculated composition of the vapor phase was to change the expression for f in equation 9 for DME. Using this method gives good results, but is pure-empirical and non-physical since the model matchs the vapor-pressure of pure DME well. Therefore it does not seem possible to model the N_2 systems with the current model, but more work is needed.

4.2.8 Results for systems with N_2 and CO_2

Figure 22 shows the model results for the five component system: N_2/CO_2/DME/H_2O/methanol. As can be seen the prediction of the L1 phase is good while the vapor phase has problems for N_2. Prediction for the L2 phase are not good and shows sattering. As for all the other calculations an average of the experimental data are used as feed to the flash. And the uncertainty of the data is reflected in the output of the flash. The model also finds a second liquid phase at the last point while none was found experimentally. The reason to this is that the system is not fixed and changing the feed will make the second liquid phase disaper. More data and more work on the model is therefore needed before the 5 component systems can be modeled in a satisfactory manner.

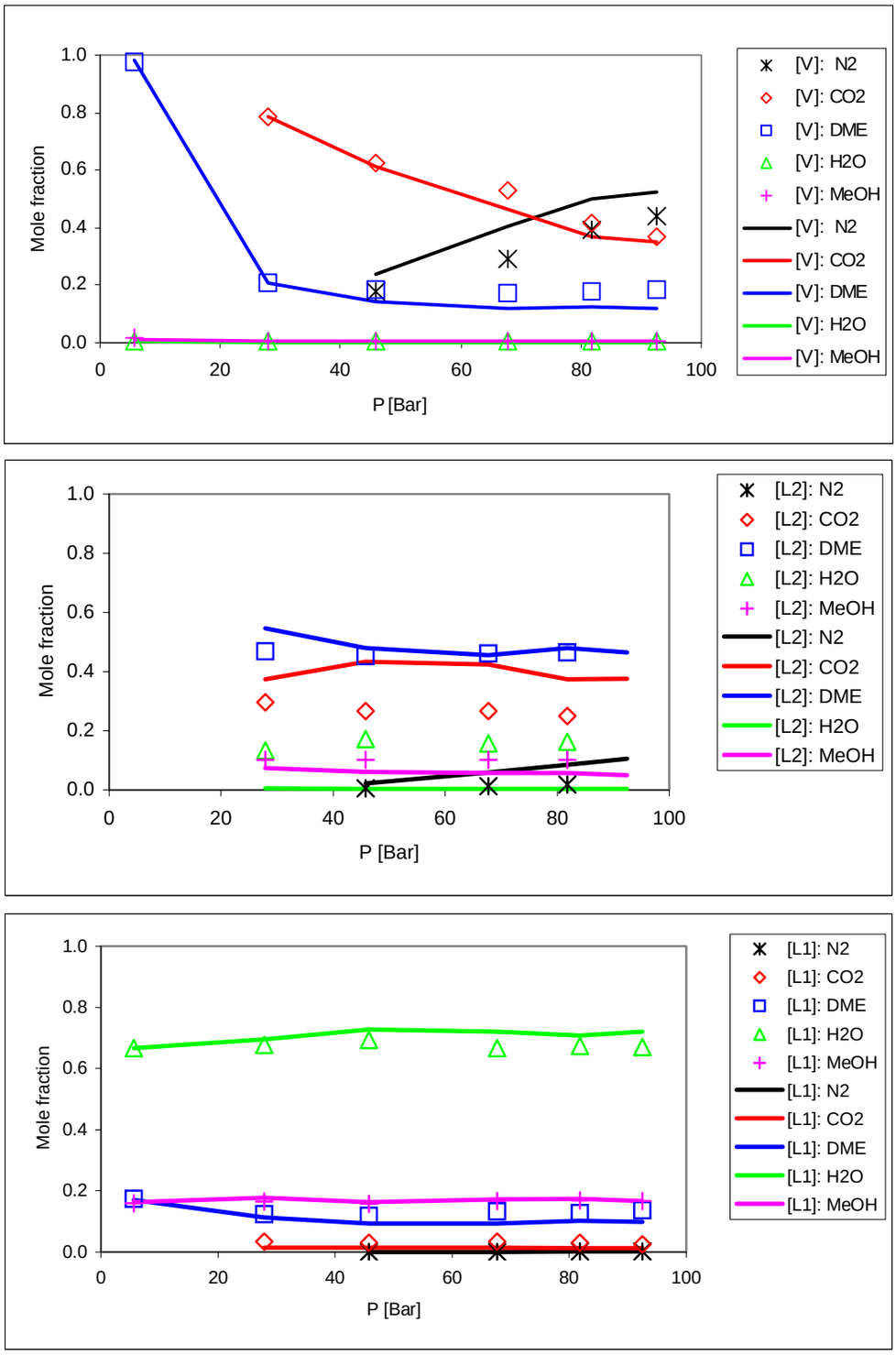

Figure 22: Plot of model + experimental data for the system: N_2/CO_2/DME/H_2O/methanol, T=35.0°C, L1: Lower liquid phase, L2: Upper liquid phase, V: vapor phase

5 Conclusion

This project has proved that it is possible to measure both VLE and VLLE systems on a routine basis, that allows a full isotherm to be measured in one week with 8 – 13 data points. This has been obtained by treating the experimental methods as production as opposed to research. Each step is done exactly the same way each time and all the steps possible have been automatic. By far the biggest gain in time has been obtained by using pure component calibration combined with on-line sampling. This has reduced the time used for calibration from being a matter of working days to zero, since the calibration can be done in between sampling from the cell.

As a result 41 isotherms have been measured and published or submitted for publication, 32 of these systems have not previously been published, and 18 were VLLE systems.

Some of the data has been modelled using the SRK equation of state combined with the Mathias-Copeman expression for the vapor pressure. A linear mixing rule was used for the b-parameter and the MHV1 mixing rule was used for the a-parameter combined with the NRTL model for the excess Gibbs energy. The α parameter in the NRTL model was fixed to 0.2 and no temperature dependences were found necessary for the τ_{ij} parameter. Therefore only two parameters were fitted for each binary pair. When using the model to predict multi component systems using a multiphase flash, very good results were obtained for systems with CO_2, while the model has some problems with systems including N_2. The basis and solution for the deviation of the model for systems with N_2 have not been found.

6 List of symbols

a, b Equation of state parameters for mixtures
F_{OB} Object function
g Gibbs energy
N Number of components
D Number of data points
n Molenumber
P Pressure
q Mixing rule constant of MHV1
R Universal gas constant
x, y, z Mole fractions
V Molar volume
T Temperature

Greek letters
α Dimensionless mixture parameter
λ Interactions parameter

Superscripts
E Excess Gibbs energy
cal Calculated value
exp Measured value

Subscripts
ii Pure component
ij Interaction parameter
ci Critical constant for component i
ri Reduced value for component i
k Data point number
L Liquid phase
V Vapor phase

7 References

Abrams, D.S.; Prausnitz, J.M. Statistical Thermodynamics of Liquid Mixtures: A new Expression for the Excess Gibbs Energy of Partly of Completely Miscible Systems. AIChE J., **1975**, *21*, 116-128

Angus, S.B.; Armstrong, B.; de Reuck, K.M. Carbon dioxide. International Thermodynamic Tables of the Fluid State –3, IUPAC, Pergamon Press: Oxford **1976**.

Angus, S.B.; Armstrong, B.; de Reuck, K.M. Nitrogen. International Thermodynamic Tables of the Fluid State –6, IUPAC, Pergamon Press: Oxford **1979**.

Brunner, E.; Hultenschmidt, W.; Schlichthärle, G. Fluid Mixtures at High Pressures IV. Isothermal Phase Equilibria in Binary Mixtures Consisting of (Methanol + Hydrogen or Nitrogen or Methane or Carbon Monoxide or Carbon Dioxide) J. Chem. Thermodynamics **1987**, *19*, 273-291.

Chang, E.; Calado, J. C. G.; Streett, W. B. Vapor-Liquid Equilibrium in the System Dimethyl Ether
/Methanol from 0 to 180 C and Pressures to 6.7 MPa. J. Chem. Eng. Data, **1982**, *27*, 293-298 .

Chang, C.J.; Day, C.; Ko, C.; Chiu, K. Densities and P-x-y Diagrams for Carbon Dioxide Dissolution in Methanol, Ethanol, and Acetone Mixtures. Fluid Phase Equilibria **1997**, *131*, 243-258.

Dahl, S.; Fredenslund, A.; Rasmussen, P. The MHV2 Model: A UNIFAC-Based Equation of State
Model for Prediction of Gas Solubility and Vapor-Liquid Equilibria at Low and High Pressures. Ind. Eng. Chem. Res. **199**1, *30*(8), 1936-1945.

T.E. Daubert, R.P. Danner, DIPPR; Physical and thermodynamic properties of pure compounds, Data compilation, Hemiphere Publishing Corparation, New York, 1989.

Design Institute for Physical Property Data (DIPPR), AIChE, *1989*.

Duschek, W.; Kleinrahm, R.; Wagner, W. Measurement and correlation of the (pressure, density, temperature) relation of nitrogen in the temperature range from 273.15 to 323.15 K at pressures up to 8 MPa. J. Chem. Thermodynamic, **1988**, 20, 1069-1077.

Elbaccouch, M.M; Elliott, J.R. High-Pressure Vapour-Liquid Equilibrium for Dimethyl Ether + Ethanol and Dimethyl Ether + Ethanol + Water. J. Chem. Eng. Data **2000**, *45*, 1080-1087.

Hall, D. J.; Mash, C. J.; Pemberton, R. C. “Title” Nat. Phys. Lab. (U.K.), Rep. Chem.,

1979, 95.

Hansen, J.B.; Voss, B.; Joensen, F.; Sigurdardottir, I. Large Scale Manufacture of Dimethyl Ether – A new alternative diesel fuel from natural gas. SAE Paper No. 950063, **1995**.

Haworth, W.S.; Sutton, L.E.; Equilibrium of Polar Gases. Transactions of the Faraday Society **1971**, *586* (67), 2901-2914.

Holldorff, H.; Knapp, H. Binary Vapour-Liquid-Liquid Equilibrium of Dimethyl Ether – Water and Mutual Solubilities of Methyl Chloride and Water. Fluid Phase Equilibria **1988**, *44*, 195-209.

Japas, M. L.; Franck, E. U. "Title" Ber. Bunsen-Ges. Phys. Chem., **1985**, *89*, 793.

Jonasson, A.; Persson, O.; Fredenslund, Aa. High-Pressure Solubility of Carbon Dioxide and Carbon Monoxide in Dimethyl Ether. J. Chem. Eng. Data **1995**, *40*, 296-300.

Jonasson, A.; Persson, O.; Rasmussen, P. High-Pressure Solubility of Hydrogen in Dimethyl Ether. J. Chem. Eng. Data **1995**, *40*, 1209-1210.

Katayama,T.; Ohgaki,K.; Maekawa, G.; Goto, M.; Nagano,T. Isothermal Vapour-Liqid Equilibria of Acetone-Carbon Dioxide and Methanol-Carbon Dioxide Systems at High Pressures. J. Chem. Eng. Japan **1975**, *8*, 89-92.

Kooner, Z. S.; Phutela, R. C.; Fenby, D. V. "Title" Aust. J. Chem., **1980**, *33*, 9.

Krichevskii, I. R.; Lebedeva, "Title" E. S. Zh. Fiz. Khim., **1947**, *21*, 715.

Kurihara, K.; Minoura, T.; Takeda, K.; Kojima, K. Isothermal Vapor-Liquid Equilibria for Methanol + Ethanol + Water, Methanol + Water, and Ethanol + Water. J. Chem. Eng. Data, **1995**, *40*, 679-684

Larsen, B.L.; Rasmussen, P.; Fredenslund, A. A modified UNIFAC group-contribution model for prediction of phase equilibria and heats of mixing, Ind. Eng. Chem. Res. **1987**, *26*, 2274-2286

Laursen, T.; Rasmussen, P.; Andersen S.I. VLE and VLLE measurements of dimethyl ether containing systems. J. Chem. Eng. Data. **2002a**, *47* (2), 198-202.

Laursen, T.; Andersen S.I. High-Pressure Vapor-Liquid Equilibrium for Nitrogen + Methanol. Accepted by J. Chem. Eng. Data., **2002b**

Laursen, T.; Andersen S.I. VLE and VLLE measurements of dimethyl ether containing systems II. Submitted to J. Chem. Eng. Data. **2002c**

Laursen, T.; Andersen, S.I. Måling af multifaseligevægte. Dansk Kemi, **2002d**, 83(4),

29-31 (Note: Non-reviewed article in danish)

Laursen, T.; Andersen, S.I. Modellering af multifaseligevægte. Dansk Kemi, **2002e**, 83(6), 29-31 (Note: Non- reviewed article in danish)

McGlashan, M. L.; Williamson, A. G. Isothermal Liquid-Vapour Equilibria for System Methanol-Water. J. Chem. Eng. Data, **1976**, *21* (2), 196-199.

Mathias, P.M.; Copeman, T.W. Extension of the Peng-Robinson Equation of State to Complex Mixtures: Evaluation of the various Forms of the Local Composition Concept. Fluid Phase Equilib. **1983**, *13*, 91-108.

Michelsen, M.L. The Isothermal Flash Problem. Part 1. Stability
Fluid Phase Equilibria, **1982**, 9, 1-9.

Michelsen, M.L. A modified Huron-Vidal Mixing Rule for Cubic Equations of State. Fluid Phase Equilibria, **1990**, *60*, 213-219

Muller, G.; Bender, E. Maurer, G. Das Dampf-Flussigkeitsgleich wicht des ternaeren Systems Ammoniak/Kohlendioxid/Wasser bei Hoben Wassergehalten im Bereich Zwischen 373 und 473 Kelvin. Ber. Bunsenges. Phys. Chem., **1988**, *92*. 148-160.

Nakayama, T.; Sagara, H.; Arai, K.; Saito, S. High Pressure Liquid-Liquid Equilibria for the System of Water, Ethanol and 1,1-Difluoroethane at 323.2K. Fluid Phase Equilibria, **1987**, *38*, 109-127.

Ohgaki, K.; Katayama, T. Isothermal Vapour-Liquid Equilibria Data for Binary Systems Containing Carbon Dioxide at High Pressures: Methanol-Carbon Dioxide, n-Hexane-Carbon Dioxide, and Benzene-Carbon-Dioxide Systems. J. Chem. Eng. Data **1976**, *21*(1), 53-55.

Pozo, M.; Streett, W. Fluid Phase Equilibria for the system Dimethyl ether\water from 50 to 220 and pressures to 50.9 MPa. J. Chem. Eng. Data, **1992**, *37*, 306-310.

Renon, H.; Prausnitz, J.M. Local Compositions in Thermodynamic Excess Functions for Liquid Mixtures. AIChE J., **1968**, *14* (1), 135

Rigby, M.; Prausnitz, J. M. Solubility of Water in Compressed Nitrogen, Argon and Methane J. Phys. Chem., **1968**, *72*, 330.

G. Soave, Equilibrium Constants from a Modified Redlich-Kwong Equation of State, Chem. Eng. Sci. **1972**, *27*, 1197-1203

Teodorescu, M.; Rasmussen, P. High-Pressure Vapour-Liquid Equilibria in the systems: Nitrogen + Dimethyl ether, Methanol + Dimethyl ether, Carbon Dioxide + Dimethyl ether + Methanol and Nitrogen + Dimethyl ether + Methanol. J. Chem. Eng. Data. . J. Chem. Eng. Data **2001**, *46* (3), 640-646.

Weber, W; Zeck, S.; Knapp, H. Gas Solubilities in Liquid Solvents at High Pressures: Apparatus and Results for Binary and Ternary Systems of N_2, CO_2 and CH3OH. Fluid Phase Equilibria.
1984, *18*, 253-278.

8 Appendix A: 1. Article

VLE and VLLE measurements of dimethyl ether containing systems.

Torben Laursen, Peter Rasmussen and Simon Ivar Andersen*
Engineering Research Centre IVC-SEP, Department of Chemical Engineering, The Technical University of Denmark, DK-2800 Lyngby Denmark
Corresponding author, e-mail: sia@kt.dtu.dk

Abstract
The present work describes a method that allows rapid measurement of both VLE and VLLE isotherms. Samples of the various phases are taken from a high-pressure autoclave equipped with windows using a movable needle. The samples are sent directly into a GC that is calibrated using pure compounds. The procedure allows for the measurement of a full isotherm with 5 to 10 data points for all phases during one working week. The method has been validated by measuring the systems CO_2+CH_3OH and CO_2+$(CH_3)_2O$, and compared with literature data. Thereafter a range of systems composed of the five components N_2, CO_2, $(CH_3)_2O$, H_2O, CH_3OH has been measured at 25.0, 35.0 and 45.0°C. This work contains new experimental data for the systems: CO_2+CH_3OH, N_2+$(CH_3)_2O$, CO_2+$(CH_3)_2O$, N_2+$(CH_3)_2O$+H_2O, CO_2+$(CH_3)_2O$+H_2O, CO_2+$(CH_3)_2O$+H_2O+CH_3OH, N_2+$(CH_3)_2O$+H_2O+CH_3OH, and N_2+CO_2+$(CH_3)_2O$+H_2O+CH_3OH, in the temperature range of 25 to 45°C and pressure range of 3 to 105 bar.

Introduction
Dimethyl ether ($(CH_3)_2O$) (DME) may have a future as a replacement for engine fuel obtained from fossil reserves.[1] In order to produce DME on a large scale, a full knowledge of the many phase equilibria involved is required. Previously a number of VLE data have been published[2,3,4,5], but the only VLLE data found are for the system $(CH_3)_2O$+H_2O limited to 8 bar.[6] This work focuses on the phase behaviour found in systems, made by combinations of the 5 components: N_2, CO_2, $(CH_3)_2O$, H_2O, CH_3OH, since all five components are involved when producing DME. Some of these systems show both VLE and VLLE behaviour while others show only VLE in the experimental pressure and temperature ranges. The equipment used allows for measurement of the composition of all the phases present in the cell, and new data are presented for 8 different combinations of the five components.

Experimental section
The experimental apparatus is based on a high-pressure autoclave equipped with two windows, a movable sample needle and valves for performing on-line sampling from the cell. The equipment can be used to measure both VLE and VLLE, but not LLE, for safety reasons.
A schematical outline of the equipment can be found in Figure 1.

Equilibrium cell. The vapor-liquid equilibrium measurements are done in a TOP autoclave model number 1030.0000 with a volume of 570 mL. It is equipped with 2 sapphire windows for observation of the cell content. Stirring is carried out mechanically. The stirrer is mounted through the lid of the cell, and is driven using a magnetic coupling (Maxon DC motor model P10). The temperature is measured using a Eurotherm 2416 PT100 with a resolution of ϒ0.1 K placed in a well in the cell, and through the lid. Pressure is measured by using a MEX3D20B35 from Bourdon with a resolution of ϒ0.1 bars. Thermostating is obtained using 4 heating rods mounted into the side of the autoclave, and additional heating on the top of the lid of the autoclave.

Sample needle. The autoclave is equipped with a movable sample needle from Top Industries, so that samples can be taken from any liquid phase present in the cell. The sample needle is constructed similar to a manual bicycle pump, taking advantage of a difference in piston area in order to operate over a large pressure difference. The needle is held in place using compressed air, and by adjusting the pressure of the compressed air to a level that just matches the pressure in the cell given the area difference, the needle can be moved using little force and without any leaks.

Pump. The circulation of the liquid is achieved using a pump of type LEWA FC M400.

Sampling Valves. The system is equipped with 3 Rheodyne sample valves, all placed in series with a He stream that enters the GC. The liquid valve (Model 7410) is equipped with a 0.5 μL loop, and the vapour valve (model 7010) is mounted with a 500 μL loop. The calibration valve (Model 7410) is not mounted with a loop of fixed size. The maximum operating temperature and pressure of the liquid and vapour valves are 125°C, 340 bars and 150°C, 340 bars respectively.

Gas Chromatograph (GC). The samples taken were analysed using a Carlo Erba HRGC 5300 GC equipped with a TCD detector (HWD 430). The columns used were 3 m 1/8 inch stainless steel with 2.1 mm I.D. filled with HayeSep T mesh 80/100. The oven and injection zone temperature was set to 140°C, the He flow to 19 $mL \cdot min^{-1}$ for the analysis-column and 19 $mL \cdot min^{-1}$ for the reference-column. Both flows are set at an oven temperature of 70°C. The TCD was set to 200°C and the filaments to 220°C.

GC Calibration. Calibration of the GC was performed by injecting different amounts of the pure component, and making a regression of the amount versus the area, see Figure 2. When the compound is a liquid at room conditions a manual SEG 1.0 μL syringe was used to inject samples in the range of 0.1 to 1.0 μL in order to make the calibration curve. The numbers used are an average of two injections. It was found that if the syringe used was equipped with a plunger-support, the standard deviation of the injection would be on average 0.5% and about 5% without, so all liquid calibrations were done using a plunger-support.

If the compound is a gas, loops in the size range of 10 to 500 μL were used. The loops are mounted onto the calibration valve. The sample was taken from a gas cylinder and flows through the loops and into a water beaker. The loops used were calibrated using pure water combined with gravimetry. The uncertainty of the size of the loop was found to be within 0.5μL. The numbers used are an average of two injections, and the standard deviation was on average 0.1%.

This method of calibration requires that the density of the compound is known at the condition where the calibration is performed. The density of DME was taken from Haworth and Sutton.[7] The density of water and methanol was taken from DIPPR.[8] The

density of CO_2 was taken from Angus et al.[9] and the density of N_2 was taken from Angus et al.[10]

Sampling from the autoclave. When taking a liquid sample, the height of the sampling needle was adjusted so that the tip of the needle was located in the liquid phase that was to be measured. Liquid was recycled using the liquid pump through the liquid sampling valve. When turning the liquid sampling valve, the liquid sample entered the He stream and was carried into the GC.

Vapor samples were taken through a hole in the lid and were led to the on-off valve and vapour valve by a 1/16 inch pipe. Both the pipe and valves were heated to 20 kelvins above the temperature of the autoclave to ensure that no liquid dropout occurred when taking samples from the cell. The loop was filled with sample by letting vapor from the cell flow through it and into a beaker filled with water until the pipe and valve were flushed. When turning the vapor valve the vapor sample enters the He stream and was carried into the GC. For all points 2 samples were taken and an average was used as the result. The deviation between the points was normally within 1 to 2% while for points measured at the detection limit of the GC would show a deviation up to 50%.

Uncertainty. The uncertainty of the measured molefractions is estimated to be 3%, while the reproducibility was found to be within 1.5 %. The uncertainty was found to depend on which phase was measured. The vapor had the smallest uncertainty averaging 1% for the light component and on average 25% for the heavy components. The large number for the heavy components was due to the small amount present in the vapor phase, leading to measurements close to the limit of the used GC-detector. The liquid phases were found to have an average uncertainty of 3%. The uncertainty of the temperature was found to be 0.2 K, while the uncertainty of the pressure measurements was found to be 0.1 bar.

Procedures. The system was evacuated for several hours before use to remove any traces of gas. Liquid samples were added to the cell using the vacuum to draw the liquid into the cell. When there was to be water in the cell, sufficient water was added so that it's level would reach above the lower window edge to ensure that any phase split could be seen. The gasses were added from high-pressure supply bottles. When CO_2 was needed at pressures above about 55 bars an ISCO pump model 260D Syringe Pump, was used to supply the desired pressure. After adding the compounds, the autoclave was thermostated overnight and samples were taken from each phase as described above. The next point was reached by adding either CO_2 or N_2 to the system until the desired pressure level was reached. After reaching the pressure, the cell contents would be mixed for 10 minutes and left for a minimum 2 hours to reach equilibrium. Depending on the separation time needed on the GC, either 1 or 2 points could be measured each day. The calibration did not take any additional time since it was done while the system was awaiting equilibrium.

Materials. The materials used are listed in Table 1. The purity of the materials was checked using GC, and they were used without any further purification.

Results and discussion

In order to test the equipment and procedure, two well-known systems were measured at first. Figure 3 shows a comparison between measured data and 4 sets of literature data for the system CO_2+CH_3OH at 25.0°C. The measured data are given in Table 2. Good agreement was obtained, but due to the large scatter of the data available for this

system, the system CO_2+$(CH_3)_2O$ was also measured in order to verifiy the equipment and method. Figure 4 shows a comparison between literature data and data obtained in this work for the system CO_2+$(CH_3)_2O$ at 47.0°C. As can be seen, good agreement was achieved. The measured data are given in Table 3.

Following the verification, the system N_2+$(CH_3)_2O$ was measured. This system shows only VLE behaviour. The measured data are given in Table 4.
The system N_2+$(CH_3)_2O$ +H_2O shows VLLE behaviour, see Table 5. N_2 has little effect on the composition of the two liquid phases while the vapor phase becomes enriched in N_2.

The system CO_2+$(CH_3)_2O$ +H_2O shows VLLE behavior due to the poor miscibility between water and DME, see Figure 5 and Table 6. When performing these measurements, the water rich phase showed little change when increasing the pressure by adding CO_2 to the cell, while the DME rich phase expands, until the system was at the limit of becoming an LLE system.

The system N_2+$(CH_3)_2O$+H_2O+CH_3OH showed only VLE behaviour. This was believed to be due to the amount of methanol in the system, see Table 7. As the numbers show, the only major changes when increasing the pressure is the lowering of the DME mole fraction in the vapor phase. The liquid phase showed only minor changes.

The system CO_2+$(CH_3)_2O$+H_2O+CH_3OH showed both VLE and VLLE behavior, see Table 8. Before CO_2 was added to the cell, a VLE system was found due to the presence of methanol. When CO_2 was added, a second liquid phase would split out. As the pressure was increased by adding CO_2 to the cell, the DME content of the water rich liquid phase was found to decrease. The vapor phase became richer in CO_2; the same was found in the DME rich liquid phase. As the pressure was increased the DME rich liquid phase would expand until the system was on the limit of becoming an LLE system and the measurement was stopped.

The system N_2+CO_2+$(CH_3)_2O$+H_2O+CH_3OH was measured by adding water, methanol and DME to the cell. CO_2 was then added until a second liquid phase split out. Thereafter the pressure was increased by adding N_2, see Table 9. It was seen in the cell that the DME rich phase would become smaller when the pressure was increased, and in some cases the system would revert to a VLE system at elevated pressures

Conclusions
Equipment for measuring both VLE and VLLE phase equilibria has been developed. It has been demonstrated that the use of on-line sampling combined with pure-component calibration can provide both fast and reliable experimental data. The method has been validated by measuring the system CO_2+$(CH_3)_2O$ at 47.0° and the system CO_2+CH_3OH at 25.0, 30.0, and 40.0°C. The measured data show good agreement with literature data. Isotherms at 25.0, 35.0, 45.0°C, are presented for the systems: N_2+$(CH_3)_2O$, N_2+$(CH_3)_2O$+H_2O, CO_2+$(CH_3)_2O$+H_2O, CO_2+$(CH_3)_2O$+H_2O+CH_3OH, N_2+$(CH_3)_2O$+H_2O+CH_3OH, and N_2+CO_2+$(CH_3)_2O$+H_2O+CH_3OH, of these only N_2+$(CH_3)_2O$ has previously been published.

Literature Cited

(1) Hansen, J.B.; Voss, B.; Joensen, F.; Sigurdardottir, I. Large Scale Manufacture of Dimethyl Ether – A new alternative diesel fuel from natural gas. SAE Paper No. 950063, 1995.

(2) Jonasson, A.; Persson, O.; Fredenslund, Aa. High-Pressure Solubility of Carbon Dioxide and Carbon Monoxide in Dimethyl Ether. J. Chem. Eng. Data **1995**, *40*, 296-300.

(3) Jonasson, A.; Persson, O.; Rasmussen, P. High-Pressure Solubility of Hydrogen in Dimethyl Ether. J. Chem. Eng. Data **1995**, *40*, 1209-1210.

(4) Teodorescu, M.; Rasmussen, P. High-Pressure Vapour-Liquid Equilibria in the systems: Nitrogen + Dimethyl ether, Methanol + Dimethyl ether, Carbon Dioxide + Dimethyl ether + Methanol and Nitrogen + Dimethyl ether + Methanol. J. Chem. Eng. Data. . J. Chem. Eng. Data **2001**, *46*, 3, 640-646.

(5) Holldorff, H.; Knapp, H. Binary Vapour-Liquid-Liquid Equilibrium of Dimethyl Ether – Water and Mutual Solubilities of Methyl Chloride and Water. Fluid Phase Equilibria **1988**, *44*, 195-209.

(6) Elbaccouch, M.M; Elliott, J.R. High-Pressure Vapour-Liquid Equilibrium for Dimethyl Ether + Ethanol and Dimethyl Ether + Ethanol + Water. J. Chem. Eng. Data **2000**, *45*, 1080-1087.

(7) Haworth, W.S.; Sutton, L.E.; Equilibrium of Polar Gases. Transactions of the Faraday Society **1971**, 586 (67), 2901-2914.

(8) Design Institute for Physical Property Data (DIPPR), AIChE, 1989.

(9) Angus, S.B.; Armstrong, B.; de Reuck, K.M. Carbon dioxide. International Thermodynamic Tables of the Fluid State –3, IUPAC, Pergamon Press: Oxford 1976.

(10) Angus, S.B.; Armstrong, B.; de Reuck, K.M. Nitrogen. International Thermodynamic Tables of the Fluid State –6, IUPAC, Pergamon Press: Oxford 1979.

(11) Chang, C.J.; Day, C.; Ko, C.; Chiu, K. Densities and P-x-y Diagrams for Carbon Dioxide Dissolution in Methanol, Ethanol, and Acetone Mixtures. Fluid Phase Equilibria **1997**, *131*, 243-258.

(12) Ohgaki, K.; Katayama, T. Isothermal Vapour-Liquid Equilibria Data for Binary Systems Containing Carbon Dioxide at High Pressures: Methanol-Carbon Dioxide, n-Hexane-Carbon Dioxide, and Benzene-Carbon-Dioxide Systems. J. Chem. Eng. Data **1976**, *21*, 1, 53-55.

(13) Katayama,T.; Ohgaki,K.; Maekawa, G.; Goto, M.; Nagano,T. Isothermal Vapour-Liqid Equilibria of Acetone-Carbon Dioxide and Methanol-Carbon Dioxide Systems at High Pressures. J. Chem. Eng. Japan **1975**, *8*, 89-92.

(14) Brunner,E.; Hultenschmidt,W.; Schlichthärle, G. Fluid Mixtures at High Pressures IV. Isothermal Phase Equilibria in Binary Mixtures Consisting of (Methanol + Hydrogen or Nitrogen or Methane or Carbon Monoxide or Carbon Dioxide) J. Chem. Thermodynamics **1987**, *19*, 273-291.

(15) Tsang, C.Y.; Streett, W.B.; Vapour-Liquid Equilibrium in the System Carbon Dioxide/Dimethyl Ether. J. Chem. Eng. Data **1981**, *26*, 155-159.

The authors wish to thank Haldor Topsøe A/S for financial support of the project.

Table 1. Materials Used, Supplier and Purity

Material	Supplier	Purity in %
Carbon dioxide	Hede Nielsen	99.995
Nitrogen	Hede Nielsen	99.995
Dimethyl ether	Sigma Aldrich	99.7
Water	J.T. Baker	99.998
Methanol	J.T. Baker	99.8

Table 2. Composition of the Liquid (x_1) and Vapor (y_1) phase at the Pressure P for the System CO_2 (1) + CH_3OH (2)

x_1	y_1	P/bar	x_1	y_1	P/bar
		T=25.0°C			
0.0946	0.9824	13.0	0.4799	0.9901	51.3
0.2061	0.9873	26.8	0.5399	0.9897	54.4
0.3667	0.9902	43.5	0.5379	0.9895	54.2
		T=30.0°C			
0.0748	0.9756	12.4	0.4662	0.9888	54.8
0.2032	0.9871	30.8	0.4586	0.9893	55.0
0.1951	0.9875	30.7	0.4552	0.9896	55.1
0.3248	0.9896	44.8			
		T=40.0°C			
0.0887	0.9799	15.9	0.3448	0.9894	53.8
0.1693	0.9871	28.8	0.4251	0.9883	63.4
0.2486	0.9889	41.4			

Table 3. Composition of the Liquid (x_1) and Vapor (y_1) Phase at the Pressure P for the System CO_2 (1) + $(CH_3)_2O$ (2)

x_1	y_1	P/bar	x_1	y_1	P/bar
		T=25.0°C			
0.0000	0.0000	6.0	0.6164	0.8875	34.6
0.2597	0.6857	16.6	0.7261	0.9190	41.2
0.4546	0.8179	25.6	0.8478	0.9542	49.8
		T=35.5°C			
0.0000	0.0000	7.9	0.4289	0.7874	31.1
0.1023	0.4052	13.0	0.5491	0.8476	38.8
0.1954	0.5821	17.7	0.6515	0.8791	45.8
0.2272	0.5908	19.3	0.7154	0.8986	50.8
0.3443	0.7292	25.7	0.7939	0.9221	57.3
		T=47.0°C			
0.0000	0.0000	10.3	0.5932	0.8218	50.3
0.0708	0.2862	14.5	0.6536	0.8476	55.9
0.1412	0.4432	18.7	0.8140	0.8886	73.2
0.2590	0.5992	25.6	0.7869	0.8769	69.7
0.3880	0.7106	34.3	0.7414	0.8684	64.1
0.4768	0.7651	40.4			

Table 4. Composition of the Liquid (x_1) and Vapor (y_1) Phase at the Pressure P for the System N_2 (1) + $(CH_3)_2O$ (2)

x_1	y_1	P/bar	x_1	y_1	P/bar
		T=25.0°C			
0.0000	0.0000	6.0	0.0667	0.8366	61.9
0.0096	0.5462	15.1	0.0808	0.8472	72.3
0.0196	0.6863	23.4	0.0935	0.8531	82.9
0.0294	0.7483	31.9	0.1038	0.8572	91.4
0.0415	0.7971	41.7	0.1178	0.8619	102.4
0.0550	0.8245	52.6			
		T=35.0°C			
0.0000	0.0000	7.8	0.0706	0.7971	65.8
0.0092	0.4716	16.5	0.0824	0.8054	73.1
0.0174	0.5962	23.2	0.0947	0.8155	82.9
0.0255	0.6745	30.7	0.1112	0.8207	95.3
0.0385	0.7352	41.1	0.1243	0.8240	103.5
0.0529	0.7723	52.6			
		T=45.0°C			
0.0000	0.0000	10.0	0.0488	0.6997	49.0
0.0052	0.2735	15.0	0.0630	0.7300	58.9
0.0121	0.4488	20.9	0.0812	0.7559	72.8
0.0220	0.5599	28.3	0.0969	0.7667	83.0
0.0308	0.6230	34.9	0.1116	0.7756	92.8
0.0384	0.6599	40.4	0.1265	0.7796	102.1

Table 5. Composition of the Liquid 1 (x_1, x_2), Liquid 2 (x_1, x_2) and Vapor (y_1, y_2) Phase at the Pressure P for the System N_2 (1) + $(CH_3)_2O$ (2) + H_2O (3)

Lower liquid		Upper liquid		Vapour		P/bar
x_1	x_2	x_1	x_2	y_1	y_2	
			T=25.0°C			
0.0000	0.1468	0.0000	0.8580	0.0000	0.9978	5.6
0.0003	0.1704	0.0037	0.8455	0.4744	0.5224	19.2
0.0004	0.1613	0.0108	0.8402	0.6734	0.3249	41.5
0.0006	0.1561	0.0178	0.8491	0.7269	0.2714	60.5
0.0008	0.1503	0.0265	0.8384	0.7548	0.2398	80.7
0.0012	0.1500	0.0363	0.8427	0.7691	0.2289	98.5
			T=35.0°C			
0.0000	0.1448	0.0000	0.8318	0.0000	0.9913	7.3
0.0001	0.1477	0.0023	0.8134	0.3219	0.6705	16.8
0.0001	0.1491	0.0044	0.8235	0.4426	0.5514	23.7
0.0003	0.1458	0.0085	0.8166	0.5655	0.4268	36.7
0.0004	0.1403	0.0140	0.8308	0.6318	0.3629	51.3
0.0005	0.1373	0.0194	0.8197	0.6705	0.3266	64.8
0.0008	0.1348	0.0259	0.8141	0.6950	0.3006	81.2
0.0012	0.1426	0.0354	0.8273	0.7083	0.2878	99.6
			T=45.0°C			
0.0000	0.1317	0.0000	0.8139	0.0000	0.9921	9.4
0.0001	0.1346	0.0028	0.8213	0.2878	0.7046	20.4
0.0003	0.1309	0.0097	0.8327	0.5046	0.4887	41.0
0.0006	0.1272	0.0174	0.8255	0.5981	0.3992	61.4
0.0008	0.1247	0.0264	0.8183	0.6341	0.3621	80.5
0.0010	0.1180	0.0368	0.8271	0.6479	0.3486	99.3

Table 6. Composition of the Liquid 1 (x_1, x_2), Liquid 2 (x_1, x_2) and Vapor (y_1, y_2) Phase at the Pressure P for the System CO_2 (1) + $(CH_3)_2O$ (2) + H_2O (3)

Lower liquid		Upper liquid		Vapour		P/bar
x_1	x_2	x_1	x_2	y_1	y_2	
			T=25.0°C			
0.0000	0.1793	0.0000	0.7231	0.0000	0.9900	5.4
0.0098	0.1100	0.1538	0.7231	0.5739	0.4230	11.8
0.0129	0.0664	0.3575	0.5991	0.7845	0.2141	20.7
0.0272	0.0462	0.5484	0.4259	0.8661	0.1316	29.5
0.0349	0.0280	0.6916	0.2898	0.9117	0.0856	39.4
0.0428	0.0160	0.7945	0.1661	0.9480	0.0520	48.6
			T=35.0°C			
0.0000	0.1142	0.0000	0.8274	0.0000	0.9900	7.5
0.0080	0.0862	0.2172	0.7142	0.6264	0.3644	19.0
0.0164	0.0546	0.4434	0.5227	0.7909	0.1982	31.7
0.0163	0.0288	0.6443	0.3207	0.8727	0.1171	46.0
0.0234	0.0154	0.7867	0.1688	0.9138	0.0732	58.8
			T=45.0°C			
0.0000	0.1309	0.0000	0.7683	0.0000	0.9900	9.4
0.0068	0.0886	0.1899	0.7270	0.5622	0.4262	21.4
0.0116	0.0483	0.4189	0.5435	0.7514	0.2425	36.2
0.0155	0.0358	0.5451	0.4303	0.8092	0.1857	45.7
0.0179	0.0133	0.6498	0.3156	0.8528	0.1432	55.9
0.0180	0.0194	0.6828	0.2452	0.8701	0.1243	61.9

Table 7. Composition of the Liquid (x_1, x_2, x_3) and Vapor (y_1, y_2, y_3) Phase at the Pressure P for the System N_2 (1) + $(CH_3)_2O$ (2) + H_2O (3) + CH_3OH (4)

Liquid			Vapour			P/bar
x_1	x_2	x_3	y_1	y_2	y_3	
			T=25.0°C			
0.0000	0.2359	0.6358	0.0000	0.9897	0.0031	4.8
0.0004	0.2533	0.6241	0.5787	0.4136	0.0042	22.4
0.0011	0.2600	0.6069	0.7094	0.2816	0.0046	41.5
0.0015	0.2454	0.6262	0.7623	0.2324	0.0034	60.9
0.0020	0.2474	0.6209	0.7837	0.2103	0.0032	80.5
0.0025	0.2463	0.6229	0.7973	0.1982	0.0024	102.1
			T=35.0°C			
0.0000	0.3123	0.5308	0.0000	0.9771	0.0101	6.8
0.0005	0.3015	0.5430	0.4197	0.5654	0.0067	17.8
0.0013	0.2972	0.5469	0.6096	0.3810	0.0045	34.2
0.0019	0.3014	0.5430	0.6770	0.3146	0.0041	48.2
0.0026	0.3062	0.5373	0.7126	0.2788	0.0041	60.7
0.0037	0.3199	0.5195	0.7444	0.2497	0.0024	82.3
0.0044	0.3036	0.5444	0.7562	0.2354	0.0043	98.6
			T=45.0°C			
0.0000	0.2630	0.6392	0.0000	0.9795	0.0098	8.2
0.0006	0.2896	0.5888	0.4432	0.5399	0.0106	27.2
0.0012	0.2696	0.6290	0.5658	0.4232	0.0063	42.5
0.0017	0.2739	0.6221	0.6354	0.3544	0.0053	61.7
0.0025	0.2758	0.6177	0.6792	0.3105	0.0057	81.2
0.0031	0.2650	0.6246	0.6889	0.3007	0.0057	99.5

Table 8. Composition of the Liquid 1 (x_1, x_2, x_3), Liquid 2 (x_1, x_2, x_3) and Vapor (y_1, y_2, y_3) Phase at the Pressure P for the System CO_2 (1) + $(CH_3)_2O$ (2) + H_2O (3) + CH_3OH (4). (***: Phase not present)

Lower liquid			Upper liquid			Vapour			P/bar
x_1	x_2	x_3	x_1	x_2	x_3	y_1	y_2	y_3	
T=25.0°C									
0.0000	0.1467	0.7449	***	***	***	0.0000	0.9861	0.0061	4.6
0.0174	0.1220	0.7469	0.2339	0.5383	0.1611	0.7412	0.2469	0.0089	18.3
0.0213	0.0704	0.7748	0.4442	0.4515	0.0549	0.8507	0.1435	0.0029	27.7
0.0306	0.0313	0.8163	0.6442	0.2615	0.0611	0.9154	0.0759	0.0049	40.1
0.0434	0.0225	0.8095	0.6731	0.1844	0.1123	0.9339	0.0556	0.0074	45.2
T=35.0°C									
0.0000	0.1100	0.4145	***	***	***	0.0000	0.9797	0.0071	5.8
0.0356	0.1475	0.6607	0.2288	0.4636	0.2014	0.7451	0.2449	0.0044	24.6
0.0311	0.0802	0.7366	0.4210	0.4272	0.0740	0.8281	0.1623	0.0050	34.2
0.0282	0.0523	0.7590	0.5538	0.3363	0.0493	0.8712	0.1187	0.0048	42.5
0.0350	0.0337	0.7644	0.6883	0.2435	0.0258	0.9040	0.0856	0.0055	51.3
T=45.0°C									
0.0000	0.2073	0.6840	***	***	***	0.0000	0.9789	0.0093	8.0
0.0229	0.1745	0.6856	0.1293	0.5047	0.2767	0.6080	0.3814	0.0048	21.6
0.0281	0.0930	0.7707	0.3220	0.4515	0.1607	0.7609	0.2244	0.0091	34.9
0.0259	0.0493	0.8039	0.5292	0.3484	0.0764	0.8354	0.1533	0.0053	48.1
0.0287	0.0380	0.8087	0.6312	0.2984	0.0323	0.8607	0.1275	0.0058	55.6

Table 9. Composition of the Liquid 1 (x_1, x_2, x_3, x_4), Liquid 2 (x_1, x_2, x_3, x_4) and Vapor (y_1, y_2, y_3, y_4) Phase at the Pressure P for the System N_2 (1) + CO_2 (2) + $(CH_3)_2O$ (3) + H_2O (4) + CH_3OH (5). (***: Phase not present)

Lower liquid				Upper liquid				Vapour				P/bar
x_1	x_2	x_3	x_4	x_1	x_2	x_3	x_4	y_1	y_2	y_3	y_4	
T=25.0°C												
0.0000	0.0000	0.1697	0.6769	***	***	***	***	0.0000	0.0000	0.9845	0.0154	4.4
0.0000	0.0289	0.1266	0.6869	0.0000	0.2829	0.4873	0.1345	0.0000	0.7983	0.1966	0.0024	21.6
0.0003	0.0261	0.1136	0.7071	0.0064	0.2495	0.4692	0.1774	0.2529	0.5768	0.1663	0.0014	42.6
0.0005	0.0250	0.1241	0.6865	0.0118	0.2614	0.5107	0.1180	0.3352	0.5039	0.1562	0.0016	56.9
0.0008	0.0250	0.1250	0.6853	0.0170	0.2571	0.5126	0.1184	0.4439	0.3962	0.1544	0.0024	70.5
0.0011	0.0256	0.1300	0.6936	0.0227	0.2514	0.5168	0.1162	0.4866	0.3520	0.1551	0.0017	84.3
0.0013	0.0229	0.1298	0.6887	0.0291	0.2448	0.5230	0.1111	0.5226	0.3154	0.1561	0.0024	99.4
T=35.0°C												
0.0000	0.0000	0.1747	0.6660	***	***	***	***	0.0000	0.0000	0.9762	0.0088	5.6
0.0000	0.0343	0.1241	0.6773	0.0000	0.2963	0.4678	0.1335	0.0000	0.7837	0.2073	0.0036	27.9
0.0003	0.0310	0.1187	0.6927	0.0055	0.2676	0.4515	0.1728	0.1781	0.6247	0.1868	0.0041	45.8
0.0009	0.0343	0.1321	0.6663	0.0135	0.2665	0.4617	0.1563	0.2920	0.5271	0.1708	0.0052	67.7
0.0012	0.0296	0.1267	0.6732	0.0189	0.2509	0.4653	0.1634	0.3926	0.4139	0.1815	0.0067	81.8
0.0014	0.0254	0.1358	0.6708	***	***	***	***	0.4383	0.3672	0.1842	0.0046	92.5
T=45.0°C												
0.0000	0.0000	0.1620	0.7028	***	***	***	***	0.0000	0.0000	0.9734	0.0115	7.3
0.0000	0.0362	0.1398	0.6951	0.0000	0.2480	0.4889	0.1634	0.0000	0.7290	0.2589	0.0061	30.3
0.0003	0.0288	0.1272	0.7073	0.0061	0.2321	0.4983	0.1625	0.1725	0.5797	0.2363	0.0057	49.3

0.000	0.025	0.130	0.695	0.010	0.207	0.482	0.197	0.258	0.495	0.232	0.008	
8	7	6	2	8	0	3	7	2	5	0	3	64.5
0.000	0.024	0.130	0.687					0.316	0.446	0.224	0.007	
9	8	8	5	***	***	***	***	0	2	6	3	76.5
0.001	0.020	0.127	0.693					0.372	0.399	0.215	0.005	
2	0	7	7	***	***	***	***	2	7	2	8	94.8

Figure 1. Schematic diagram of the VLLE experimental apparatus: 1, Autoclave; 2, Window; 3, Movable liquid sample needle; 4, Mechanical stirrer; 5, Liquid sampling valve; 6, Vapour sampling valve; 7, Liquid pump; 8, Waste; 9, Heated box; 10, Heated pipe; 11, He inlet; 12, Line to GC; 13, Temperature sensor; 14, Pressure gauge; 15, Calibration sampling valve; 16, Inlet to calibration valve; 17, Waste from calibration loop; 18, Inlet to cell.

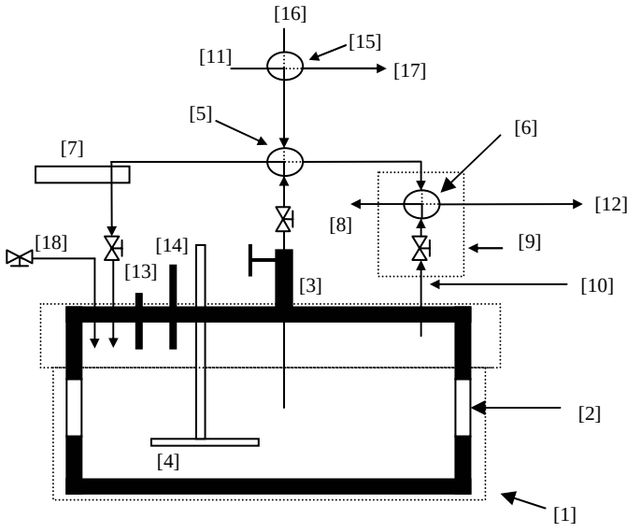

Figure 2. Example of a calibration curve for N_2, including the distribution of the points for the system N_2 (1) + $(CH_3)_2O$ (2) at 45.0 °C.

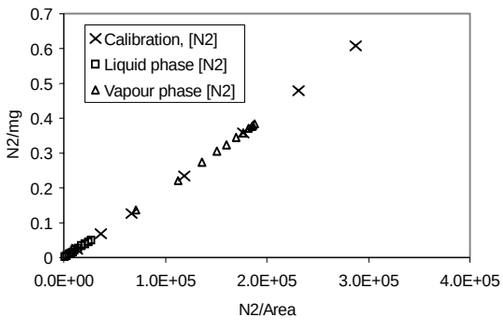

Figure 3. Comparison between literature data for the system CO_2 (1) + CH_3OH (2) at 25.0°C and data obtained in this work.

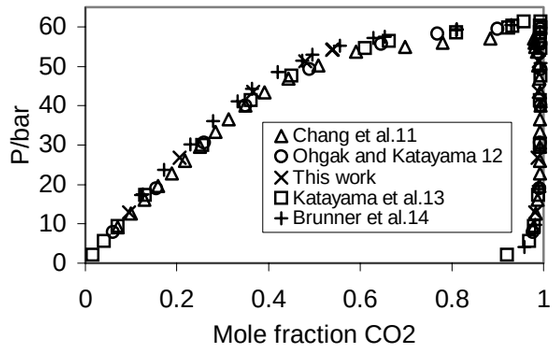

Figure 4. Comparison between literature data and data obtained in this work for the system CO_2 (1) + $(CH_3)_2O$ (2) at 47.0°C.

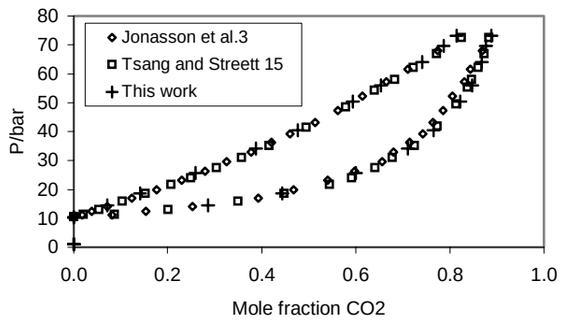

Figure 5. 3D chart showing the VLLE system CO_2 (1) + $(CH_3)_2O$ (2) + H_2O (3) at 35.0°C

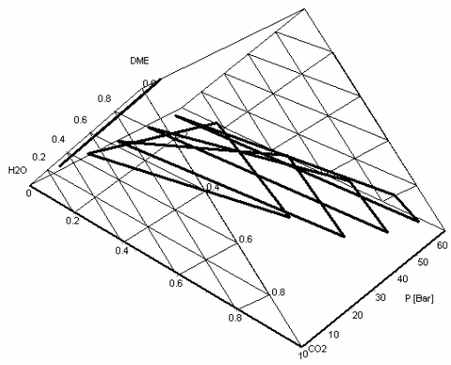

9 Appendix B: 2. Article

High-Pressure Vapor-Liquid Equilibrium for Nitrogen + Methanol

Torben Laursen* and Simon Ivar Andersen
Engineering Research Center IVC-SEP, Department of Chemical Engineering, The Technical University of Denmark, DK-2800 Lyngby Denmark
Corresponding author, e-mail: tl@kt.dtu.dk

Abstract
A number of authors have raported VLE data for the system nitrogen+methanol, but none of the publications give data for both the liquid and the vapor phases. In this work, experimental data for both the liquid and the vapor phases are presented in the temperature range 25°C to 45°C and in the pressure range 7 to 102 bars. The experimental data has been correlated using the Soave-Redlich-Kwong equation of state (SRK) combined with a k_{ij} interaction parameter.

Introduction
In a continuation of a research program involving measurements of VLE and VLLE data, the system nitrogen+methanol was measured. A number of other authors have also measured this system, but none has published data that includes both the liquid and the vapor phases. In this work the VLE system has been measured at 25, 35, 45°C in the pressure range 7 to 102 bar, including mole fractions of both the liquid and the vapor phases.

Experimental section
The measurements were previously described in details.[1] The experimental apparatus is based on a high-pressure autoclave equipped with two windows, a movable sample needle and valves for performing on-line sampling from the cell. The equipment can be used to measure both VLE and VLLE, but not LLE, for safety reasons. In the method applied, liquid samples are taken by recirculation of liquid through a liquid sampling valve, and gas samples are taken by flushing a vapor sampling valve with heated vapor from the cell.
The composition was measured using a Carlo Erba HRGC 5300 gas chromotograph based on pure component calibration. The uncertainty of the given molefractions is estimated to 0.001 molefraction.

Chemicals. Methanol with a purity of 99.8 % was obtained from J.T.Baker. Nitrogen was supplied by Hede Nielsen with a purity of 99.995 %. The purity was verified by GC analysis. The chemicals were used without any further purification.

Results and discussions
Vapor – liquid equilibrium data for nitrogen+methanol at (298.15, 308.15 and 318.15) K are presented in Table 1. The values in Table 1 show that the solubility of nitrogen in

methanol is small and is only slightly affected by the temperature, while the solubility of methanol in the vapor phase is significantly affected by the temperature, at low pressures.

Figure 1 shows a comparison between experimental data for the liquid phase obtained in this work and literature data [2-4]. The data presented in this work shows a slightly smaller solubility of nitrogen, but considering the small measured molefractions there is a fair agreement between the datasets.

The data was correlated using the Soave-Redlich-Kwong (SRK) equation of state[5] combined with the k_{ij} interaction parameter. The critical constants and the acentric factors were taken from DIPPR[6] and are given in Table 2. The parameters were fitted using equal fugacity as the object function. The parameters obtained were: $K_{12} = K_{21} = -0.1418$. Comparisons of the correlations with the measured data are shown in Figure 2-3. It is seen that the data are well correlated.

Acknowledgement

The authors appreciate the help to prepare this manuscript from Peter Rasmussen.

Literature Cited

(1) Laursen, T.; Rasmussen, P.; Andersen S.I. VLE and VLLE measurements of dimethyl ether containing systems. *J. Chem. Eng. Data.* **2002,** *47* (2), 198-202.

(2) Weber, W; Zeck, S.; Knapp, H. Gas Solubilities in Liquid Solvents at High Pressures: Apparatus and Results for Binary and Ternary Systems of N_2, CO_2 and CH_3OH. *Fluid Phase Equilibria*. **1984**, *18*, 253-278.

(3) Brunner,E.; Hultenschmidt,W.; Schlichthärle, G. Fluid Mixtures at High Pressures IV. Isothermal Phase Equilibria in Binary Mixtures Consisting of (Methanol + Hydrogen or Nitrogen or Methane or Carbon Monoxide or Carbon Dioxide) *J. Chem. Thermodynamics* **1987**, *19*, 273-291.

(4) Krichevsky, I. R.; Lebedeva, E. S. *Zh. Fiz. Khim.*, **1947**, *21*, 715.

(5) Soave,G. Equilibrium constants from a modified Redlich-Kwong equation of state, *Chem. Eng. Sci.* **1972**, *27*, 1197.

(6) Daubert, T.E; Danner,R.P. DIPPR; Physical and thermodynamic properties of pure compounds, Data compilation; Hemisphere: New York, 1989.

Table 1. Composition of the Liquid (x_1) and Vapor (y_1) phase at the Pressure P for the System N_2 (1) + CH_3OH (2)

x_1	y_1	P/bar	x_1	y_1	P/bar
		T=25.0°C			
0.0010	0.9695	6.7	0.0099	0.9944	46.2
0.0023	0.9839	13.2	0.0131	0.9958	61.6
0.0042	0.9906	21.1	0.0170	0.9962	81.3
0.0063	0.9924	31.7	0.0219	0.9963	101.9
		T=35.0°C			
0.0012	0.9443	6.8	0.0094	0.9893	43.1
0.0021	0.9685	11.8	0.0143	0.9923	62.1
0.0041	0.9796	20.4	0.0175	0.9926	80.2
0.0065	0.9874	30.8	0.0221	0.9930	101.5
		T=45.0°C			
0.0013	0.9201	7.4	0.0101	0.9837	47.0
0.0021	0.9451	11.1	0.0137	0.9866	61.9
0.0040	0.9705	21.4	0.0179	0.9882	81.9
0.0065	0.9763	30.7	0.0221	0.9895	98.5

Table 2: Critical properties, acentric factors and molar masses used

	Tc/K	Pc/MPa	W	M/ g•mol^{-1}
N_2	126.20	3.400	0.0377	28.014
CH_3OH	512.64	8.097	0.5640	32.042

Figure 1. Comparison between 3 sets of literature data and this work.

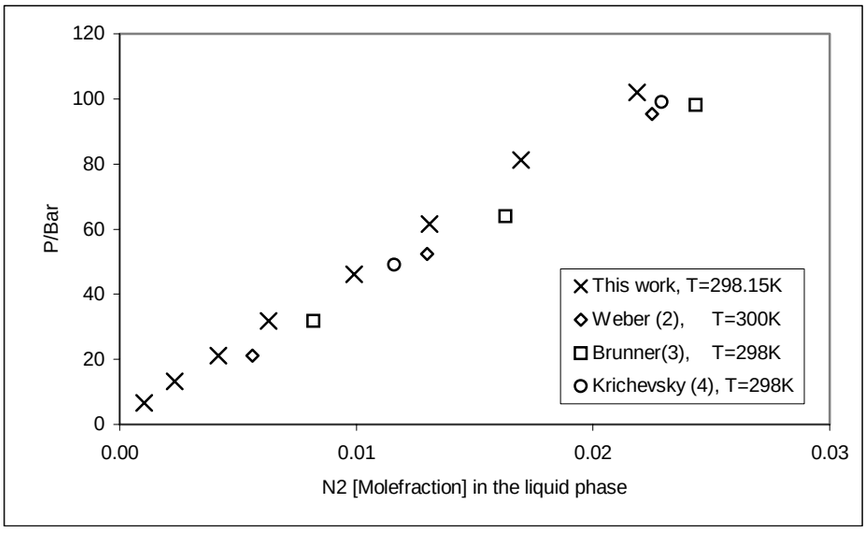

Figure 2. Pressure – composition data for nitrogen (1) + methanol (2), comparing the experimental results with model results for the liquid phases.

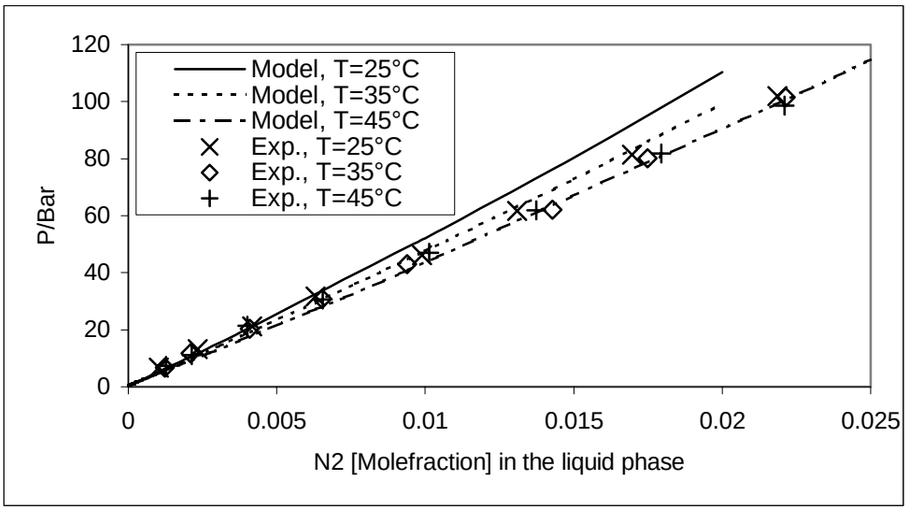

Figure 3. Pressure – composition data for nitrogen (1) + methanol (2), comparing the experimental results with model results for the vapor phases

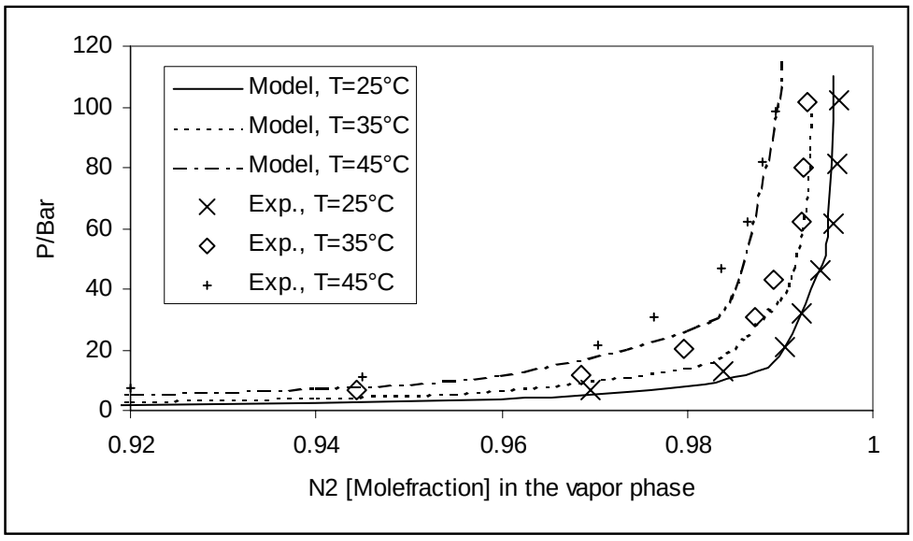

10 Appendix C: 3. Article

VLE and VLLE measurements of dimethyl ether containing systems. II

Torben Laursen and Simon Ivar Andersen*
Engineering Research Center IVC-SEP, Department of Chemical Engineering, The Technical University of Denmark, DK-2800 Lyngby Denmark
Corresponding author, e-mail: sia@kt.dtu.dk

Abstract
14 isotherms for systems composed of the components: nitrogen, carbon dioxide, dimethyl ether (DME), water, ethanol and 1-propanol have been measured. Experimental data for all the phases present, VLE or VLLE, in the temperature range 25.0°C to 45.0°C and pressure range 5 to 102 bar is presented. The data has not been correlated.

Introduction
In a continuation of a research program involving measurements of VLE and VLLE data[1,2], the systems: nitrogen + DME + water + ethanol, carbon dioxide + DME + water + ethanol, carbon dioxide + DME + ethanol, carbon dioxide + 1-propanol and carbon dioxide + DME + 1-propanol have been measured. No experimental datapoints for these systems have previously been published, except for the system carbon dioxide + 1-propanol [3,4,5]. All the systems have been measured as isotherms at the temperatures: 25.0, 35.0, 45.0°C and in the pressure range 5-102 bar. The mole fractions of both the liquid(s) and the vapor phase are given.

Experimental section
The measurements were previously described in details.[1] The experimental apparatus is based on a high-pressure autoclave equipped with two windows, a movable sampleing needle and valves for performing on-line sampling from the cell. The equipment can be used to measure both VLE and VLLE, but not LLE, for safety reasons. In the methods applied, liquid samples are taken by recirculation of liquid through a liquid sampling valve, and gas samples are taken by flushing a vapor sampling valve with heated vapor from the cell.
The composition was measured using a Carlo Erba HRGC 5300 gas chromotograph based on pure component calibration. The uncertainty of the measured mole fractions is estimated to be 3%. The uncertainty of the temperature was found to be 0.2 K, while the uncertainty of the pressure was found to be 0.1 bar.

Chemicals
The materials used are listed in Table 1. The purity of the materials was checked using GC, and they were used without any further purification.

Results and discussions
Vapor – liquid equilibrium data for nitrogen + DME + water + ethanol at (25.0, 35.0 and 45.0°C) are presented in Table 2. The system was measured by first adding water +

ethanol to the cell followed by DME. The pressure was thereafter raised by adding nitrogen to the cell. The system showed no sign of any second liquid phase, and the solubility of nitrogen in the liquid phase was small. The solubility of water in the vapor phase was so small that is could not be detected properly on the used GC.
Vapor – liquid - liquid equilibrium data for carbon dioxide + DME + water + ethanol at (25.0, 35.0 and 45.0°C) are presented in Table 3. The experimental procedure was the same was as for the prevoius system. A second liquid phase would form after raising the pressure and this second phase would expand while the vapor phase would shrink as the pressure was raised. The measurements were stopped when the system was close to being a LLE system. The solubility of water in the vapor phase was so small that it could not be detected on the used GC.
Vapor – liquid equilibrium data for carbon dioxide + DME + ethanol at (25.0, 35.0 and 45.0°C) are presented in Table 4. No second liquid phase was found. As the pressure was raised the liquid phase would expand and the measurements were stopped when the system was close to being a one phase system. Figure 1 showes a 3D plot of one of the isotherms in Table 4. The figure showes the two phases both as 2D projection lines onto the composition space and as 3D points in the composition, pressure space.
Vapor – liquid equilibrium data for carbon dioxide + 1-propanol at (35.0 and 45.0°C) are presented in Table 5. No second liquid phase was found. As the pressure was raised the liquid phase would expand and the measurements were stopped when the system was close to being a one phase system. A comparison between litterature data and the data in Table 5 is shown in Figure 2. As can be seen is there some deviation between the different datasets, but the data from this work lies close to the other datasets.
Vapor – liquid equilibrium data for carbon dioxide + DME + 1-propanol at (25.0, 35.0 and 45.0°C) are presented in Table 6. No second liquid phase was found. As the pressure was raised the liquid phase would expand and the measurements were stopped when the system was close to being a one phase system.

Acknowledgement
The authors appreciate the help to prepare this manuscript from Peter Rasmussen.

Literature Cited
(1) Laursen, T.; Rasmussen, P.; Andersen S.I. VLE and VLLE measurements of dimethyl ether containing systems. J. Chem. Eng. Data. **2002**, *47*, 2, 198-202.

(2) Laursen, T.; Andersen S.I. High-Pressure Vapor-Liquid Equilibrium for Nitrogen + Methanol. Accepted by J. Chem. Eng. Data.

(3) Vandana, V., Teja, A. S. Vapor - Liquid Equilibria in the Carbon Dioxide + 1-Propanol System
J. Chem. Eng. Data, **1995**, *40*, 2, 459-461

(4) Suzuki, K., Sue, H. , Itou, M. , Smith, R.L. , Inomata, H. , Arai, K. , Saito, S. Isothermal vapor-liquid equilibrium data for binary systems at high pressures. Carbon dioxide-methanol, carbon dioxide-ethanol, carbon dioxide-1-propanol, methane-ethanol, methane-1-propanol, ethane-ethanol, and ethane-1-propanol systems. J. Chem. Eng. Data, **1990**, *35*, 4, 63-66

(5) Yaginuma, R., Nakajima, T., Tanaka, K., Kato, M. Volumetric properties and vapor-liquid equilibria for carbon dioxide + 1-propanol system at 313.15 K. Fluid Phase Equilibria, **1998**, *144*, 203-210.

Table 1. Materials Used, Supplier and Purity

Material	Supplier	Purity in %
Carbon dioxide	Hede Nielsen	99.995
Nitrogen	Hede Nielsen	99.995
Dimethyl ether	Sigma Aldrich	99.7
Water	J.T. Baker	99.998
Ethanol	Danisco A/S	99.9
1-propanol	Merck	99.5

Table 2. Composition of the liquid (x_i) and vapor (y_i) phases at the pressure P for the VLE system nitrogen (1) + DME (2) + water (3) + ethanol (4)

Liquid			Vapor			P/bar
x_1	x_2	x_3	y_1	y_2	y_3	
			T=25.0°C			
0.0000	0.2854	0.6271	0.0000	0.9975	0.0000	4.9
0.0005	0.2860	0.6265	0.4448	0.5541	0.0000	14.3
0.0009	0.2956	0.6162	0.5756	0.4233	0.0000	21.7
0.0018	0.2929	0.6162	0.6877	0.3114	0.0000	36.1
0.0026	0.2945	0.6121	0.7435	0.2553	0.0000	50.7
0.0035	0.2923	0.6151	0.7719	0.2273	0.0000	66.7
0.0043	0.2871	0.6183	0.7878	0.2113	0.0000	80.0
0.0054	0.2883	0.6177	0.7980	0.2011	0.0000	102.1
			T=35.0°C			
0.0000	0.2921	0.6188	0.0000	0.9978	0.0000	6.2
0.0005	0.2948	0.6147	0.3422	0.6560	0.0000	14.3
0.0010	0.2945	0.6153	0.5090	0.4900	0.0000	23.2
0.0018	0.2902	0.6171	0.6270	0.3717	0.0000	37.1
0.0026	0.2882	0.6197	0.6834	0.3152	0.0000	50.9
0.0038	0.2905	0.6174	0.7283	0.2708	0.0000	66.7
0.0043	0.2836	0.6213	0.7468	0.2524	0.0000	81.7
0.0055	0.2806	0.6231	0.7652	0.2340	0.0000	101.9
			T=45.0°C			
0.0000	0.2416	0.6555	0.0000	0.9966	0.0000	7.3
0.0002	0.2376	0.6513	0.2023	0.7952	0.0000	11.7
0.0006	0.2474	0.6395	0.4163	0.5750	0.0000	21.0
0.0012	0.2403	0.6447	0.5609	0.4371	0.0000	33.8
0.0019	0.2387	0.6460	0.6477	0.3511	0.0000	47.7
0.0028	0.2347	0.6475	0.6995	0.2992	0.0000	66.5
0.0035	0.2296	0.6525	0.7267	0.2721	0.0000	80.1
0.0043	0.2293	0.6508	0.7456	0.2529	0.0000	101.4

Table 3. Composition of the liquid (x_i) and vapor (y_i) phase at pressure P for the VLLE system: carbon dioxide (1) + DME (2) + water (3) + ethanol (4)

Lower liquid			Upper liquid			Vapor			P/bar
X_1	x_2	x_3	x_1	x_2	x_3	y_1	y_2	y_3	
				T=25.0°C					
0.0000	0.2396	0.7164				0.0000	0.9985	0.0000	5.1
0.0152	0.1549	0.7869	0.1305	0.5200	0.3002	0.6413	0.3583	0.0000	14.1
0.0174	0.1163	0.8249	0.2491	0.5260	0.1813	0.7572	0.2425	0.0000	19.6
0.0205	0.0668	0.8730	0.3909	0.4277	0.1473	0.8385	0.1609	0.0000	26.7
0.0180	0.0394	0.9040	0.5480	0.3525	0.0734	0.8900	0.1092	0.0000	34.8
0.0214	0.0334	0.9082	0.5803	0.2907	0.1057	0.9044	0.0946	0.0000	37.9
				T=35.0°C					
0.0000	0.2577	0.6178				0.0000	0.9938	0.0000	5.3
0.0227	0.2250	0.6310				0.5811	0.4179	0.0000	13.9
0.0525	0.2031	0.6292				0.7381	0.2607	0.0000	22.0
0.0521	0.1427	0.6993	0.1925	0.3109	0.3764	0.8174	0.1819	0.0000	29.5
0.0420	0.0946	0.7683	0.3241	0.3230	0.2452	0.8532	0.1456	0.0000	35.6
0.0380	0.0664	0.7978	0.4279	0.3023	0.1773	0.8789	0.1199	0.0000	40.4
				T=45.0°C					
0.0000	0.2412	0.6568				0.0000	0.9972	0.0000	7.4
0.0242	0.2408	0.6348				0.5319	0.4668	0.0000	16.2
0.0416	0.2380	0.6220				0.6440	0.3548	0.0000	21.3
0.0682	0.2281	0.6072				0.7214	0.2771	0.0000	27.7
0.0399	0.1408	0.7320	0.1673	0.3408	0.3893	0.7474	0.2515	0.0000	31.3
0.0345	0.1035	0.7786	0.2525	0.3571	0.2931	0.7906	0.2081	0.0000	36.2
0.0336	0.0756	0.8101	0.3529	0.3375	0.2226	0.8344	0.1642	0.0000	42.4

Table 4. Composition of the liquid (x_i) and vapor (y_i) phase at pressure P for the VLE system carbon dioxide (1) + DME (2) + ethanol (3)

x_1	x_2	y_1	y_2	P/bar	x_1	x_2	y_1	y_2	P/bar
				T=25.0°C					
0.0000	0.5601	0.0000	0.9883	4.2	0.2915	0.3974	0.8269	0.1701	21.7
0.1153	0.4991	0.6411	0.3542	11.2	0.3521	0.3698	0.8591	0.1381	25.5
0.2242	0.4387	0.7846	0.2120	17.6	0.4538	0.3132	0.8904	0.1068	31.8
				T=35.0°C					
0.0000	0.5319	0.0000	0.9846	5.3	0.2876	0.3832	0.8202	0.1761	26.5
0.0722	0.4921	0.5100	0.4811	10.7	0.3509	0.3504	0.8517	0.1452	31.1
0.1490	0.4558	0.6901	0.3050	16.2	0.4103	0.3181	0.8711	0.1256	35.7
0.2235	0.4162	0.7712	0.2239	21.7					
				T=45.0°C					
0.0000	0.4715	0.0000	0.9863	6.1	0.2168	0.3700	0.7755	0.2198	26.3
0.0551	0.4435	0.4675	0.5243	11.5	0.2708	0.3473	0.8168	0.1793	31.3
0.1032	0.4231	0.6197	0.3744	15.8	0.3486	0.3133	0.8521	0.1441	38.0
0.1638	0.3965	0.7226	0.2719	21.4					

Table 5. Composition of the Liquid (x_1) and Vapor (y_1) Phase at the Pressure P for the system carbon dioxide (1) + 1-propanol (2)

x_1	y_1	P/bar	x_1	y_1	P/bar
		T=35.0°C			
0.0185	0.9864	4.7	0.3385	0.9970	48.5
0.0359	0.9924	8.2	0.4068	0.9943	54.7
0.0848	0.9964	16.3	0.4142	0.9961	55.7
0.1508	0.9968	25.6	0.5281	0.9957	64.3
0.2202	0.9964	35.7	0.6765	0.9952	69.1
		T=45.0°C			
0.0200	0.9855	5.4	0.2892	0.9966	49.2
0.0534	0.9934	12.1	0.3502	0.9964	56.7
0.0836	0.9958	18.4	0.4428	0.9949	66.6
0.1276	0.9964	25.0	0.5269	0.9923	73.7
0.1657	0.9965	32.2	0.7001	0.9876	83.3
0.2276	0.9971	40.5			

Table 6. Composition of the liquid (x_i) and vapor (y_i) phase at pressure P for the VLE system carbon dioxide (1) + DME (2) + 1-propanol (3)

x_1	x_2	y_1	y_2	P/bar	x_1	x_2	y_1	y_2	P/bar
				T=25.0°C					
0.0000	0.5901	0.0000	0.9950	4.3	0.2792	0.4459	0.8120	0.1865	21.6
0.1024	0.5518	0.5998	0.3980	10.8	0.3597	0.3953	0.8577	0.1409	27.2
0.2118	0.4872	0.7564	0.2420	17.2	0.3734	0.3827	0.8790	0.1197	31.3
				T=35.0°C					
0.0000	0.1741	0.0000	0.9949	5.2	0.2232	0.4294	0.7695	0.2288	22.6
0.0836	0.4987	0.5623	0.4345	11.9	0.2810	0.4012	0.8128	0.1852	27.0
0.1429	0.4842	0.6840	0.3136	16.3	0.3523	0.3624	0.8474	0.1509	32.3
				T=45.0°C					
0.0000	0.5707	0.0000	0.9937	6.3	0.1813	0.4552	0.7219	0.2756	22.7
0.0600	0.5037	0.4304	0.5615	12.2	0.2480	0.4160	0.7774	0.2203	29.2
0.1246	0.4763	0.6367	0.3599	18.0	0.3160	0.3770	0.8176	0.1801	35.1

Figure 1. A 3D plot of the isotherms for the VLE system: carbon dioxide/DME/ethanol at T=35.0°C. Projections: liquid phase: (–), vapor phase: (---).

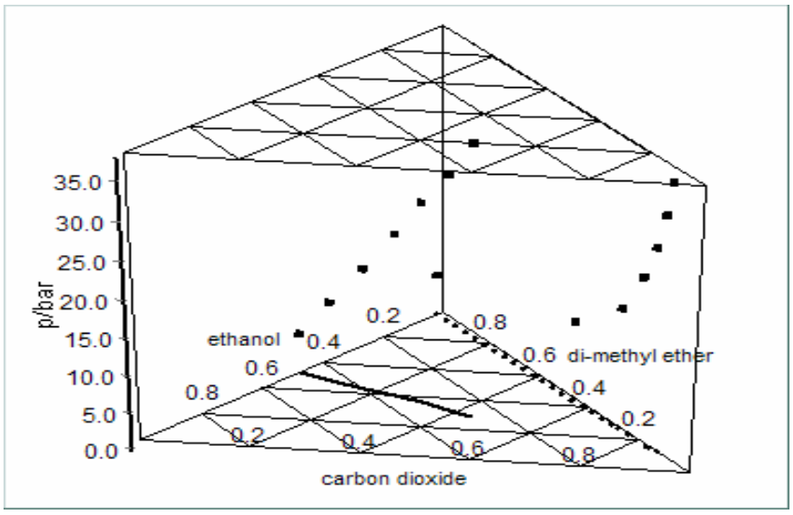

Figure 2. VLE curves for the system: carbon dioxide [1] + 1-propanol [2] taken from different sources.

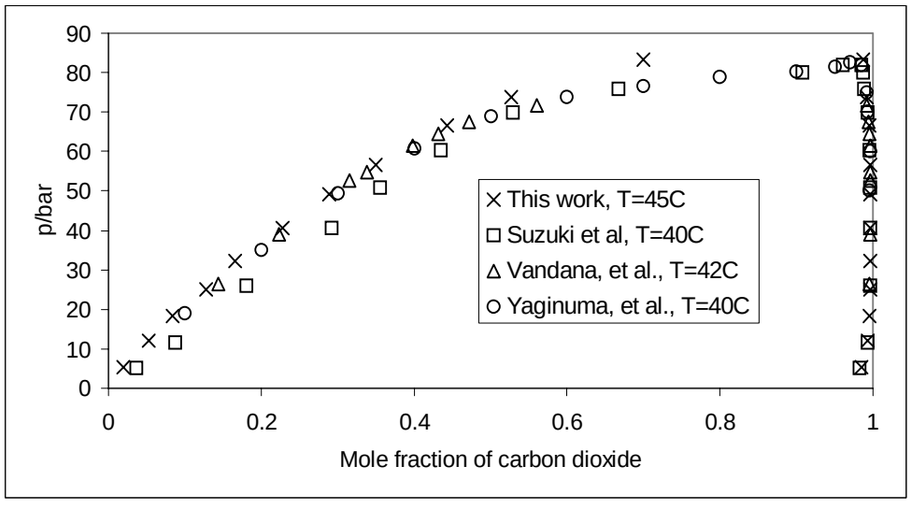

11 Appendix D: 4. Article

This article is not a non-reviewed articled published in the Danish magazine: Dansk Kemi.

Måling af multifase ligevægte: Sammensætning, tryk, temperatur og sikkerhed

Torben Laursen, Peter Rasmussen, Simon Ivar Andersen
IVC-SEP, Institut for Kemiteknik, Danmarks Tekniske Universitet, Bygning 229, 2800 Lyngby

Hvad er multifase ligevægte?
Faseligevægte findes overalt i naturen, for eksempel er der i en flaske sodavand ligevægt mellem en vandig fase og en gasfase altså et VLE system (vapor – liquid – equilibria). En andet kendt eksempel er en blanding af madolie og vand, her dannes to væskefaser og man har et LLE system (liquid – liquid– equilibria).
Hvis man blander madolie i en flaske sodavand vil man have to væskefaser og en gasfase, et VLLE system (vapor – liquid – liquid– equilibria), som er et eksempel på et multifase system. Når der måles på multifase systemer, måler man hvor mange faser der er ved en bestemt temperatur og tryk og sammensætningen af faserne.

Hvorfor måle multifase ligevægte?
En væsentlig grund til at måle multifase systemer er, at der findes meget begrænset og spredt litteratur omkring emnet. Det har været betragtet som værende meget dyrt og tidskrævende at foretage disse målinger. Derfor er både den akademiske forståelse og den industrielle anvendelse af multifase systemer nærmest ikke eksisterende, og man må derfor forvente, at der ligger store ubenyttede resourcer gemt i emnet.
Når en kemisk proces planlægges til en fabrik, er det meget vigtigt at man allerede i design fasen ved hvor mange faser der dannes når kemikalier blandes og/eller reagerer. Haldor Topsoe har udviklet en proces til syntese af DME(di-methyl ether) og havde mistanke om at der var risiko for mere end en væskefase under visse driftsbetingelser. Haldor Topsøe bad derfor IVC-SEP gruppen på Institut for Kemiteknik, DTU foretage nogle målinger for at be-eller af-kræfte dette, da en sådan måling ikke er mulig i et pilot anlæg.

Udstyr
Processen hos Haldor Topsøe foregår ved tryk op til 100 bar, så for at at kunne måle både VLE og VLLE, er det nødvendigt at have en højtryks celle, som kan klare tilsvarende fysiske betingelser. For at kunne se hvor mange faser, der er i cellen, er det nødvendigt at have vinduer i cellen og for at kunne udtage en prøve fra alle de faser, som måtte findes i cellen, er det nødvendigt med et bevægeligt prøveudtag. Et design med et fikseret prøveudtag f.eks. midt i cellen kan ikke anvendes, idet man ikke på forhånd kan vide, hvor fasegrænserne findes. Figur 1 viser en skitse af udstyret.

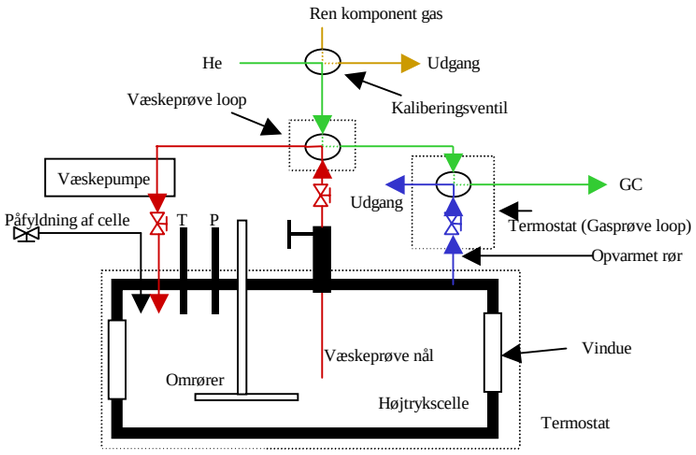

Figur 1: Skitse af højtrykscellen og tilhørende prøveudtag

Udtagning af prøve

I dette projekt analyseres de forskellige fasers sammensætning ved hjælp af en gaskromatograf (GC). Prøven som skal analyseres på GC'en bliver drevet frem af en Helium strøm, og før den når analysekolonnen er der monteret en ventil med et 0.5µL prøveloop, som anvendes til at udtage en væskeprøve og en ventil med et prøveloop på 500 µL, som anvendes til at udtage en gasprøve. Vha. en cirkulationspumpe cirkuleres væske fra den fase, som man gerne vil måle på gennem prøveloopet og ved at dreje ventilen sendes prøven direkte ind i GC'en. Gasprøven tages ved at åbne en ventil til atmosfæren og lade gasfasen komme langsomt ud gennem gasprøveloop'et. Som for væsken sendes prøven direkte ind i GC'en ved at dreje ventilen. Eneste særlige hensyn som denne metode kræver er, at det rør, som forbinder ventil med cellen, er opvarmet, for at sikre at der ikke sker kondensation i cellen. En skitse af udstyret er vist i figur 1. Linjer med grøn farve viser Heliumstrømmen. Rød farve viser væskestrømmen og blå farve viser gasstrømmen.

Analyse af prøve

For at kunne bestemme molsammensætningen af de prøver, som udtages, er det nødvendigt at kalibere GC'en. I dette projekt benyttes rene komponenter til kalibrering. Forskellige mængder af hver af de rene komponenter sendes ind i GC'en og en kaliberingskurve som giver sammenhængen mellem areal og mængder bestemmes. Hvis det er en væske, som skal kaliberes, anvendes GC injektionsnåle til at injicere prøven. Hvis det er en gas anvendes kalibrerede loops af forskellig størrelse. Kalibreringsventilen er markeret på figur 1, og den gule farve viser strømmen af kalibreringsgas. Figur 2 viser et eksempel på en kalibreringskurve for DME. De røde kryds viser kalibreringspunkterne, mens de blå punkter markerer hvor punkterne fra en række gasprøver er blevet aflæst. De sorte punkter viser hvor prøverne fra en tilhørende væskefase er blevet aflæst. Da et VLE system for Nitrogen/DME blev målt blev der bestemt en kaliberingskurve som vist for DME + en for Nitrogen.

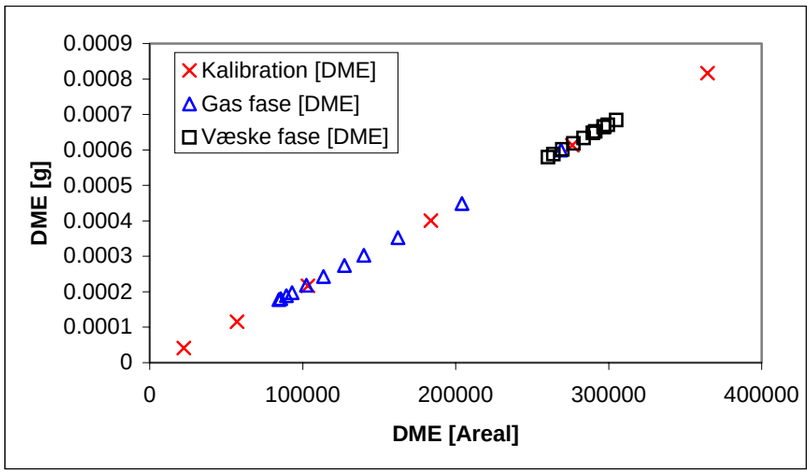

Figur 2: Eksempel på kaliberings kurve

Ved at benytte de 2 kaliberingskurver blev målingerne i figur 3 bestemt.

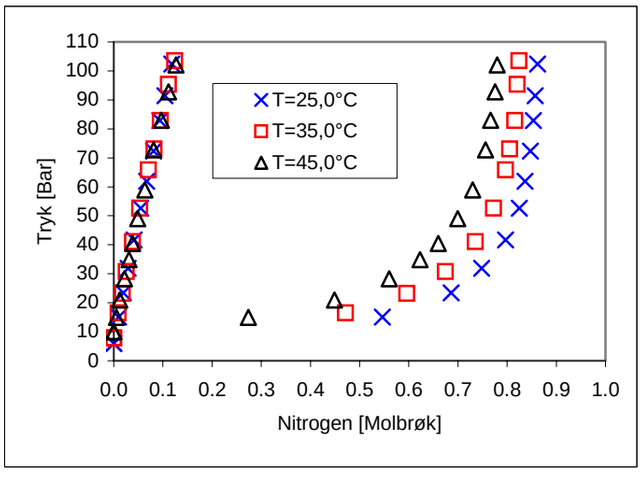

Figur 3: Eksempel på VLE målinger for blandingen: Nitrogen/DME

Sikkerhed
Målinger kræver udover almindelig laboratoriesikkerhed særlige hensyn pga. det høje tryk, som der arbejdes ved. Selve højtrykscellen er trykprøvet og udgør derfor ikke nogen sikkerhedsfare. Det samme er de ventiler, som anvendes. Alt udstyr er certificeret efter gældende sikkerhedsregler. De sikkerhedsmæssige farer opstår ved forkert brug af udstyret. Når en blanding placeres i cellen og denne termostateres vil den søge mod ligevægt, og denne ligevægt vil være ved et bestemt tryk og et bestemt antal faser med bestemte sammensætninger. For brugeren af cellen er det meget vigtigt altid at være bevidst om at disse fire variable er forbundet, så hvis der ændres på den ene, vil de tre andre automatisk ændre sig, så systemet igen er i ligevægt. Hvis brugeren f.eks. ved en

fejl hæver temperaturen meget i cellen, vil trykket følge med op, og sikkerhedsventilen kan sprænges. Det er udstyret designet til og der skulle derfor ikke kunne ske nogen personskade. Men hvis sprængstykket ikke er placeret hensigtmæssigt kan sprængningen give høreskader på nærtstående personer. En anden meget væsentlig sikkerhedsfare opstår, når der åbnes til cellen. Når en gas udvider sig, vil den blive koldere, og nogle gasser kan bliver meget kolde. F.eks. vil CO_2 blive så kold at der vil blive dannet tøris som har en temperatur omkring –60°C. Så hvis brugeren pludselig åbner en ventil til en celle med CO_2 under tryk, vil enden af udgangsrøret blive meget kold og kan sprutte med tøris. Tøris på huden eller i et øje vil give brandsår.
En anden mulig sikkerhedsfare ligger i den kraft som komprimeret gas besidder. Hvis f.eks. et rør er tryksat og det adskilles ved en fitting vil gassen strømme ud, hvilket kan få røret til at bevæge sig kraftigt og ramme omkringstående objekter med stor kraft. Den gyldne regel, når der arbejdes med højtryk, er, at der skal altid skal arbejdes eftertænksomt, og alle ændringer skal ske langsomt.

Eksempler på resultater
Som eksempler på de opnåede resultater vises N_2/DME som er et VLE system, se figur 3. Hvis der tilføjes vand til blandingen ændrer den karakter til at være et VLLE system. Et eksempel på et spændende VLLE system er vist i figur 4.

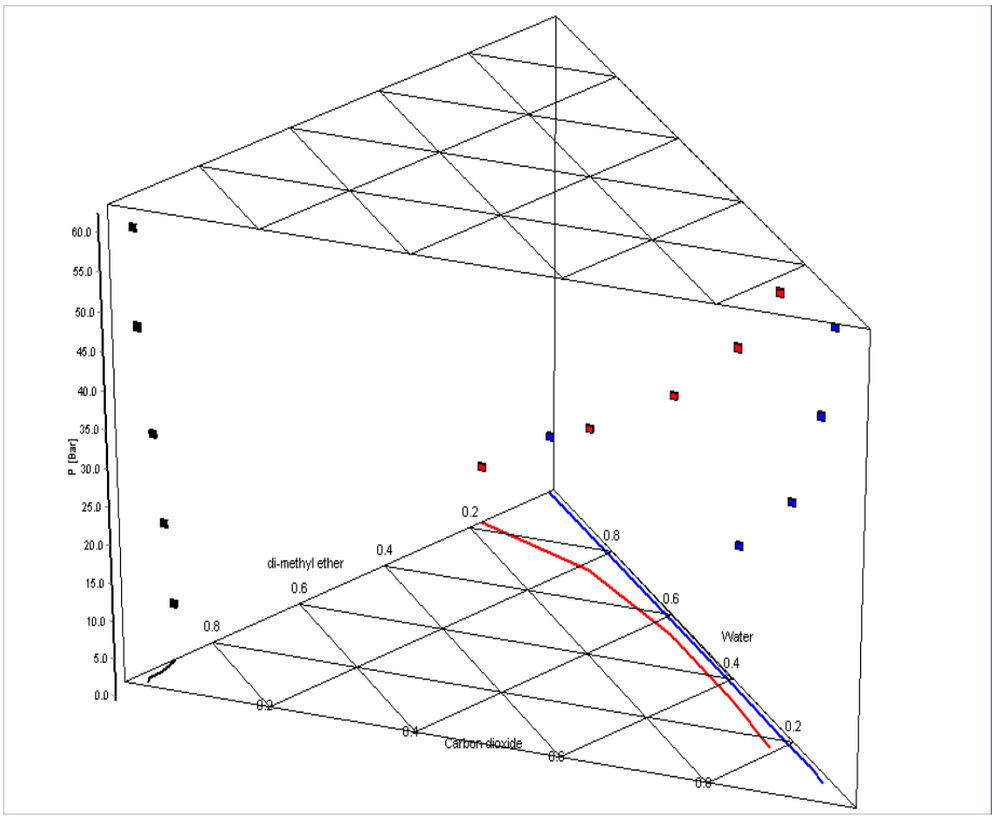

Figur 4: Eksemple på VLLE system bestående af: CO_2/DME/H_2O. Temperaturen er 35.0°C. Sort markere den den nederste væskefase, rød markere den øverste væskefase og blå gasfasen.

Systemet består af CO_2/DME/H_2O. Sammensætningen aflæses på trekanten og trykket på den lodrette akse. Temperaturen er 35.0°C. De tre punkter ved hvert tryk angiver sammensætningen af hver af de 3 faser. Figuren viser hvorledes systemet nærmer sig et tofase system når trykket hæves.
Reference listen til slut indeholder 2 artikler publiceret i dette projekt.

Videre arbejder
Det udviklede udstyr giver mulighed for en hurtig og nøjagtig måling af VLLE. Dette åbner mulighed for. At industrien kan udnytte sådanne systemer. Figur 5 viser et generelt eksempel på en process som bevæger sig mellem et VLE, VLLE og LLE ved at trykket justeres. Det kunne f.eks. være et system bestående af CO_2/DME/H_2O, ved at justere mængden af CO_2 og derved trykket er det muligt at bevæge sig mellem de 3 nævnte muligheder. En sådan process kan f.eks. anvendes til oprensning af et kemikalie eller et biologisk molekyle, se figur 5:

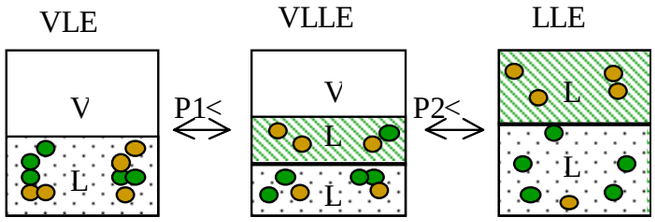

Figur 5: Skitse af generel proces. De farvede prikker angiver 2 forskellige proteiner som adskilles ved at trykket og derved antallet af faser i systemet ændres. P1, P2 og P3 angiver trykket i systemet.

På figur 5 kunne de grønne og brune pletter være to forskellige proteiner som således kunne oprenses. En anden mulighed er indenfor katalyse hvor man kunne undersøge mulighederne for at placere katalysatoren i den ene fase og oprense produktet ved at inducere en anden væskefase. Katalysatoren kunne f.eks. være en metal forbindelse eller et enzym. På nuværende tidspunkt er det kun fantasien som sætter begrænsningen.

Anderkendelse
Haldor Topsøe takkes for samarbejdet og støtte til dette projekt.

Referencer
VLE and VLLE measurements of dimethyl ether containing systems
Laursen, T., Rasmussen, P., Andersen, S.I.
Accepteret af: Journal of Chemical Engineering Data, 2001

High-Pressure Vapor-Liquid Equilibrium for Nitrogen + Methanol
Laursen, T., Andersen, S.I.
Indsendt til: Journal of Chemical Engineering Data, 2002

12 Appendix E: 5. Article

This article is not a non-reviewed articled published in the Danish magazine: Dansk Kemi.

Modellering af multifaseligevægte
Af Torben Laursen, tl@kt.dtu.dk, Peter Rasmussen, pr@kt.dtu.dk, Simon Ivar Andersen, sia@kt.dtu.dk, IVC-SEP, Institut for Kemiteknik, DTU

En kemisk blanding ved ligevægt vil bestå af et antal faser. Når en kemisk produktion planlægges og udføres, er det essentielt at kende antallet af faser og deres sammensætning som funktion af tryk og temperatur. Mængden af eksperimentelle data i litteraturen er mangelfuldt og de få data som findes må tilpasses en termodynamisk model. På basis af denne model kan man så forsøge at forudsige hvordan en blanding opfører sig i et procesrelevant temperatur- og tryk-område, hvor der ikke findes målinger. Det lyder umiddelbart ganske enkelt, men idet der kun findes mangelfulde eksperimentelle data, er det vanskelig dels at finde en egnet model og dels at få den valgte model tilpasset en given blanding. Normalt baseres modelleringsarbejdet på data fra tofase systemer, så når modellen forsøges anvendt på systemer med mere end to faser, dvs. multifase systemer, bliver modelleringsproblemet meget mere vanskeligt.

Termodynamiske modeller
Faseligevægtsberegninger kan baseres på termodynamiske tilstandsligninger. En tilstandsligning er et matematisk udtryk som giver sammenhængen mellem sammensætningen, tryk, temperatur og volumen for en kemisk blanding. En kubisk tilstandsligning kan omskrives til en 3. grads ligning i volumen. Et eksempel, den såkaldte Soave-Redlich-Kwong ligning (SRK), er vist i ligning 1:

$$P = \frac{RT}{v-b} - \frac{a}{v(v-b)} \qquad \textbf{(1)}$$

I ligning 1 er P trykket, T, temperaturen, v det molære volumen. Parametrene a og b kan let beregnes for rene stoffer ud fra stoffernes kritiske tryk og temperatur. For blandinger kan man ofte beregne parametrene ved hjælp af simple blandingsregler for renkomponentparametrene og blandingens sammensætning. For blandinger indeholdende polære og associerende komponenter viser det sig dog ikke muligt, hvis tilstandsligningen skal benyttes til nøjagtige faseligevægtsberegninger, for eksempel damp-væske ligevægt (VLE). I 1979 foreslog Huron og Vidal, at man kunne finde blandingers parametre ved hjælp af væskefasemodeller. En væskefasemodel er et matematisk udtryk, der repræsenterer en væskeblandings molære overskuds Gibbs energi (G^E), dvs. forskellen mellem den reelle molære Gibbs energi for blandingen og en molær Gibbs energi, hvis blandingen var ideal. G^E udtrykkes normalt som funktion af blandingens sammensætning, temperatur samt af to interaktionsparametre for hvert binært par i blandingen. Huron og Vidal viste, at parametren a for blandingen kan beregnes ved hjælp af ligning (2).

$$a = b\left[\sum_{i=1}^{N} x_i \frac{a_i}{b_i} - \frac{G^E}{\ln 2}\right] \quad \textbf{(2)}$$

Parametren b beregnes ved ligning 3:

$$b = \sum_{i=1}^{N} x_i b_i \quad \textbf{(3)}$$

a_i og b_i er renkomponentparametre , medens x_i er molbrøken for komponent i. Blandingen indeholder N komponenter.
Overskuds Gibbs energien, G^E beregnes i dette arbejde ved hjælp af den såkaldte NRTL model, ligning 4:

$$\frac{G^E}{RT} = \sum_{i=1}^{N} x_i \frac{\sum_{j=1}^{N} x_j \tau_{ji} \exp\left(-\alpha\ \tau_{ji}\right)}{\sum_{l=1}^{N} x_l \exp\left(-\alpha \tau_{li}\right)} \quad \textbf{(4)}$$

Ligning 4 er en funktion af molbrøker, x, og binære interaktionsenergier, τ. Parametren α, anvendes til at indregne hvor tilfældigt molekylerne blanders i blandingen. I dette arbejde benyttes α = 0.2.

Tilpasning af den termodynamiske model
For at kunne benytte en model er det først nødvendigt at kende alle de parametre, som indgår i modellen. De parametre, som er binære, dvs. afhænger af hvordan to komponenter påvirker hinanden, bestemmes ved at tilpasse modellen til eksperimentelle data. Et eksempel er vist i figur 1 for systemet nitrogen/di-methyl ether (DME).

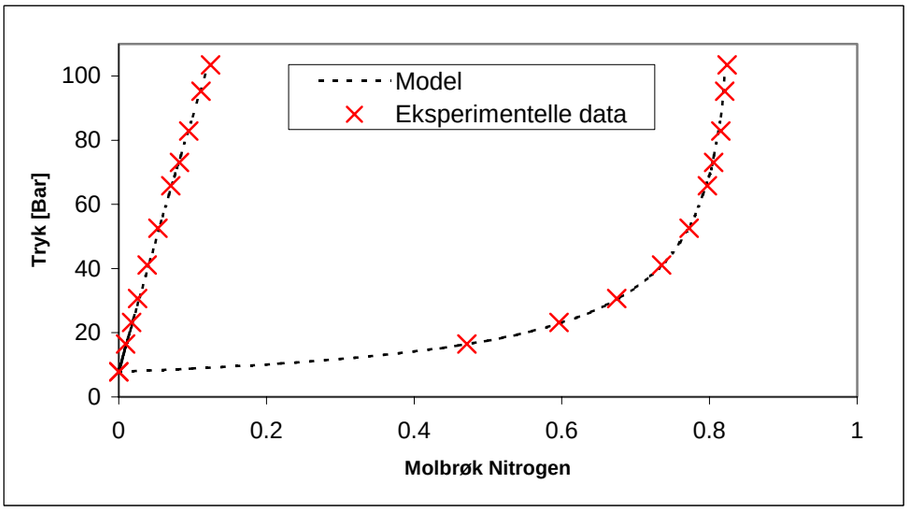

Figur 1: Eksempel på tilpasning af en termodynamiske model til systemet N_2/DME. T =

35.0°C

Figuren viser, hvorledes det er muligt at opnå en overordentlig god tilpasning af et VLE system ved at fitte de to parametre for interaktionsenergier, τ_{12} og τ_{21}, som indgår i NRTL modellen. Dette gøres for alle par i en blanding, og modellen er herefter klar til at blive anvendt på blandinger med mere end to komponenter. Man bør dog være opmærksom på, at modellen som nævnt kun er blevet tilpasset binære blandinger, og det kan derfor ikke vides, om den kan anvendes til blandinger, som har mere end to komponenter. Samtidig er den kun blevet fittet til væske-damp (VLE) data, og det kan derfor heller ikke vides, om den vil kunne beskrive en ligevægt, som f.eks. består af væske-væske-damp (VLLE).

Beregning af faseligevægte

Beregning af multifaseligevægte gøres ved hjælp af en multifaseflash. En flashroutine er i stand til at beregne antallet og sammensætningen af faser, som er i ligevægt ved givne værdier af tryk og temperatur på basis af en kendt fødeblanding. Ved givne værdier af T og P er den korrekte løsning fra multiflashroutinen antal faser og fasernes sammensætning svarende til den laveste mulige Gibbs energi. For en binær blanding kan det vises, at hvis man afbilder den molære Gibbs blandingsenergi som funktion af sammensætningen vil en tangents berøringspunkter svare til sammensætningen af de enkelte faser.

Princippet kan illusteres grafisk for systemet: DME/vand. Som x-akse haves sammensætningen og som y-akse Gibbs blandingsenergien for en given sammensætning.
Figur 2 - 4 viser principperne grafisk.

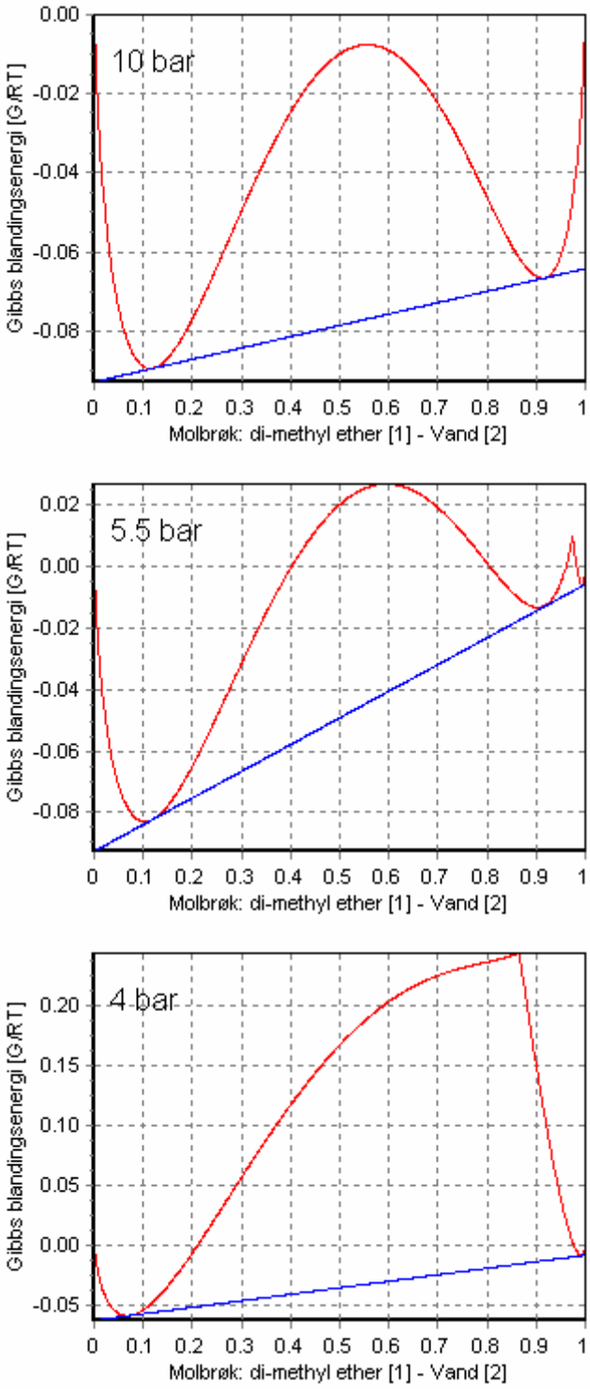

Figur 2 - 4: Eksempler på Gibbs blandingsenergi plot for systemet: DME/vand. Temperatur = 25°C. Figurene viser, hvorledes systemet bevæger sig mellem et LLE, VLLE og VLE system når trykket sænkes, fra 10 bar til 5.5 bar, og sidst til 4 bar

Figur 2 viser en tofase LLE ligevægt, i figur 3 er trykket sænket og en gas fase dannes, ligevægt består nu af et VLLE system. VLLE kan for hver temperatur kun forekomme ved et bestemt tryk. I figur 4 er trykket sænket yderligere, og den ene væskefase er nu forsvundet, og systemet er et VLE system.

Eksempler på resultater

Resultaterne i figur 2-4 stemmer overens med eksperimentelle data, og den benyttede model er således istand til at modellere både VLE, LLE og VLLE for et binært system. Figur 5-7 viser både eksperimentelle data og modelresultater for de tre faser i systemet: CO_2/DME/H_2O, ved 35°C.

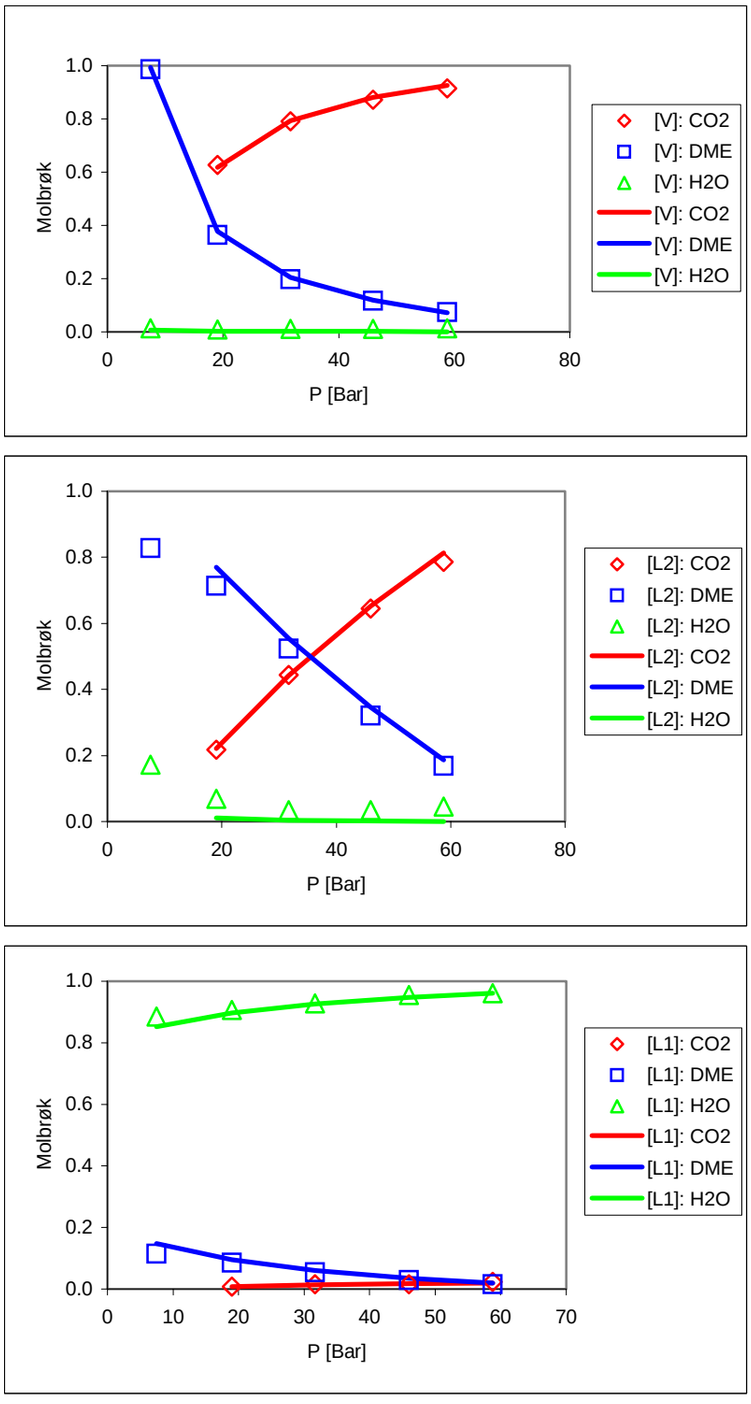

Figur 5-7: Eksperimentelle og beregnede resultater for systemet: CO_2/DME/H_2O, T=35.0°C. V: gasfase, L1: nederste væskefase, L2: øverste væskefase. Kurver: model, punkter: eksperimentelle datapunkter.

Som figurene viser, opnås et ganske godt resultat for dette system. Dette viser, at det er muligt at modellere komplicerede blandinger med en model baseret på en tilstandsligning.

Kilder

Måling af multifaseligevægte
Laursen, T., Rasmussen, P., Andersen, S.I.
Dansk Kemi 2002, 04.

VLE and VLLE measurements of dimethyl ether containing systems
Laursen, T., Rasmussen, P., Andersen, S.I.
Journal of Chemical Engineering Data, 2001, vol. 47, nr. 2, 198-202

New Mixing Rules in Simple Equation of State for Representing Vapour-Liquid Equilibria of strongly non-ideal Mixtures
Huron, M., Vidal, J.
Fluid Phase Equilibria, 1979, Vol. 3, pp. 255-271

Local Compositions in Thermodynamic Excess Functions for Liquid Mixtures (NRTL)
Renon. H., Prausnitz, J.M.
AIChE, 1968, Vol. 14, Nr. 1, pp. 135-144